Activated persulfate by iron-based materials used for refractory organics degradation: a review

Yanjiao Gao, Pascale Champagne, David Blair, Ouwen He and Tiehong Song

ABSTRACT

Recently, the advanced oxidation processes (AOPs) based on sulfate radicals (SRs) for organics degradation have become the focus of water treatment research as the oxidation ability of SRs are higher than that of hydroxyl radicals (HRs). Since the AOP-SRs can effectively mineralize organics into carbon dioxide and water under the optimized operating conditions, they are used in the degradation of refractory organics such as dyes, pesticides, pharmaceuticals, and industrial additives. SRs can be produced by activating persulfate (PS) with ultraviolet, heat, ultrasound, microwave, transition metals, and carbon. The activation of PS in iron-based transition metals is widely studied because iron is an environmentally friendly and inexpensive material. This article reviews the mechanism and application of several iron-based materials, including ferrous iron (Fe^{2+}), ferric iron (Fe^{3+}), zero-valent iron (Fe^0), nano-sized zero-valent iron (nFe^0), materials-supported nFe^0, and iron-containing compounds for PS activation to degrade refractory organics. In addition, the current challenges and perspectives of the practical application of PS activated by iron-based systems in wastewater treatment are analyzed and prospected.

Key words | advanced oxidation process, iron-based materials, persulfate, refractory organics, sulfate radicals

Yanjiao Gao (corresponding author)
Pascale Champagne
David Blair
Ouwen He
Department of Civil Engineering,
Queen's University,
Kingston K7 L 3N6,
Canada
and
Beaty Water Research Centre,
Queen's University,
Kingston K7 L 3N6,
Canada
E-mail: *tmgyj@lnut.edu.cn*

Yanjiao Gao
College of Civil Engineering and Architecture,
Liaoning University of Technology,
Jinzhou 121001,
China

Ouwen He
MOE Key Laboratory of Pollution Processes and Environmental Criteria, Tianjin Engineering Centre for Cleaner Technology of Iron-steel Industry, College of Environmental Science and Engineering,
Nankai University,
Tianjin 300350,
China

Tiehong Song
Key Laboratory of Songliao Aquatic Environment, Ministry of Education,
Jilin Jianzhu University,
Changchun 130118,
China

INTRODUCTION

In recent decades, with the increasing manufacture and the use of synthetic chemicals, a lot of wastewater containing some refractory organics is produced. Wastewater carrying these organics is usually collected by pipelines and sent to centralized wastewater treatment plants (WWTPs) for processing. However, the removal of refractory organics in the WWTPs is not complete by the biological treatment-based secondary treatment processes. It is necessary to further treat refractory organics in a more efficient way after secondary treatment processes in order to reduce the organic pollution load of the receiving water bodies.

The advanced oxidation processes (AOPs) are currently considered to be the best processes to remove refractory organics because of their strong ability to break chemical bonds of refractory organics (Fast *et al.* 2017). The AOPs initially investigated were based on hydroxyl radicals (HRs, $HO^{\bullet}$) produced *in situ* to degrade organic compounds. Two oxidants, hydrogen peroxide (H_2O_2) and ozone (O_3)

doi: 10.2166/wst.2020.190

are activated by ultraviolet (UV) or ferrous ions (Fe^{2+}) to produce HRs (Deng & Zhao 2015).The main processes consisting of H_2O_2 or O_3 are H_2O_2/UV, O_3/UV, O_3/H_2O_2/UV, and Fe^{2+}/H_2O_2 which often called the Fenton process (Csay *et al.* 2014; Ghatak 2014). Based on Fenton process, photo-Fenton (Klamerth *et al.* 2013; Pouran *et al.* 2015), electro-Fenton (Nidheesh & Gandhimathi 2012; Yahya *et al.* 2014), sono-Fenton (Ioan *et al.* 2007; Ghauch *et al.* 2011b), and sono-photo-Fenton (Babuponnusami & Muthukumar 2011) have also been extensively studied. However, the Fenton-based processes have several defects: Both H_2O_2 and O_3 are unstable, difficult to store and transport, and used in large quantities; the sludge generated in the reaction is difficult to treat; the optimal pH value is around 3.0, which will increase pH regulating agents (Neyens & Baeyens 2003).

In recent years, the AOPs based on sulfate radicals (SRs, $SO_4^{\cdot-}$) are widely studied in degradation of organic pollutants because they overcome some shortcomings of AOPs-HRs. For instance, SRs have higher oxidation potential ($E^0 = 2.5$–3.1 V) and longer half-life ($t_{1/2} = 30$–40 μs) than that of HRs ($E^0 = 1.7$–2.8 V, $t_{1/2} \leq 1$ μs), and can selectively react with unsaturated or aromatic compounds under a wide pH range of 2.0–8.0 (Olmez-Hanci & Arslan-Alaton 2013; Ike *et al.* 2018). PS ($E^0 = 2.01$ V) can be activated to produce SRs in the presence of energy (UV, ultrasonic, and heat) (Guo *et al.* 2014; Darsinou *et al.* 2015; Ji *et al.* 2015), transition metals (Fe, Co, Ni, Cu, Ag, and Mn) (Liu *et al.* 2014; Rodriguez *et al.* 2014; Zhang *et al.* 2015a, 2015b; Kang *et al.* 2018), and carbon (Cheng *et al.* 2017). Among these activators, iron has been extensively studied in activating PS to generate SRs for refractory organics degradation due to its environmental friendliness, low price and excellent activation (Matzek & Carter 2016). Prior to PS, iron was even used as stand alone technology for the removal of refractory organics among them pesticides and pharmaceuticals(Ghauch 2008; Ghauch & Tuqan 2008, 2009; Ghauch *et al.* 2009, 2010a, 2010b, 2011a). However, high concentrations of iron and iron-based materials were needed creating additional sludge formation. Therefore, researchers proposed iron use at trace level in combination with chemicals able to produce fugitive reactive oxygen species (ROS) (Ghauch 2015). Advantages of PS include chemical stability, ease of storage and transport, high solubility in water, and low cost, which broaden the application of PS in wastewater treatment (Tsitonaki *et al.* 2010). In addition, Sodium PS ($Na_2S_2O_8$) and potassium PS ($K_2S_2O_8$) are commonly used in research and pilot projects because they produce no secondary pollutants to water. Although high concentrations of sulfate species could be considered at risk which is not the case for PS concentration in the range of 0.1–20 mM (Liu & Wu 2018).

From the published literature available, some scholars have given an overview of the activated methods of sulfate radicals and their application in wastewater treatment (Zhang *et al.* 2015a, 2015b; Matzek & Carter 2016; Oh *et al.* 2016; Brienza & Katsoyiannis 2017; Wacławek *et al.* 2017; Guerra-Rodríguez *et al.* 2018; Xiao *et al.* 2018, 2019; Oh & Lim 2019). However, a detailed review about activated persulfate by iron-based materials used for refractory organics degradation has not been reported yet. Therefore, a specific and deep review on the PS activated by iron-based materials can provide state-of-the-art information for the future research of the AOPs-SRs. This paper reviews the recent advances of mechanism and application of some iron-based materials in activating PS for refractory organics degradation, and the insights towards future application of these activating methods of PS for efficient degradation of refractory organics is summarized and discussed as well.

CHARACTERIZATION METHODS OF IRON-BASED MATERIALS

In order to better understand the physicochemical properties of iron-based materials and analyze the morphology and structure of the materials, some methods of characterizing materials are necessary. There are several analytical methods such as SEM (scanning electron microscopy), TEM (transmission electron microscopy), EDS (energy dispersive system), XRD (X-ray diffraction), XPS (X-ray photoelectron spectroscopy), FTIR (Fourier transform infrared spectrometry), TGA (thermo gravimetric analysis) and BET (Brunauer-Emmett-Teller) method. The detection objects of these analysis methods are shown in Table 1.

FERROUS ION (FE^{2+}) AS ACTIVATOR

Mechanism of homogeneous activation

Ferrous ion is widely used as a homogeneous activator to react with PS to generate SRs. Usually ferrous sulfate ($FeSO_4$) and ferrous chloride ($FeCl_2$) are employed as activator to produce Fe^{2+} in solution. Naim & Ghauch (2016) demonstrated that chloride salt was more efficient toward PS activation than sulfate salt because of common ion effect on hand and because of the generation of chlorine

Table 1 | Functions of the instruments

SEM/TEM	EDS	XRD	XPS	FTIR	TGA	BET
Morphology and structure	Element and distribution	Crystalline structure	Valence state of elements	Function groups	The mass loss and thermal stability	Surface area and pore size

radicals on the second hand responsible for additional ranitidine degradation. Table 2 lists some parameters and removal rates of refractory organics treated by Fe^{2+}/PS system based on recent publications. The reaction mechanism of ferrous ion with PS to generate SRs is presented in Equation (1) (Jiang *et al.* 2013). The O–O bond of $S_2O_8^{2-}$ is cleaved to form main product $SO_4^{\bullet-}$ and byproduct SO_4^{2-} by accepting the electrons provided by Fe^{2+}, while Fe^{2+} is oxidized by the $S_2O_8^{2-}$ to become Fe^{3+}. As described in Equation (2), Fe^{2+} is produced by the reaction between $S_2O_8^{2-}$ and Fe^{3+} in the presence of $S_2O_8^{2-}$. Therefore, in a homogeneous system, there is a cycle between Fe^{2+} and Fe^{3+}. As an oxidant, $SO_4^{\bullet-}$ can also be consumed by itself or excess Fe^{2+} and $S_2O_8^{2-}$ (Equations (3)–(5)) (Kusic *et al.* 2011; Zhang *et al.* 2014), which can render a lack of $SO_4^{\bullet-}$ for organics degradation. On top of that, $SO_4^{\bullet-}$ can react slowly with H_2O to form $HO^{\bullet}$ (Equation (6)) (Olmez-Hanci *et al.* 2013).

$$S_2O_8^{2-} + Fe^{2+} \rightarrow Fe^{3+} + SO_4^{\bullet-} + SO_4^{2-} \quad (k = 15.33 M^{-1}s^{-1}) \tag{1}$$

$$S_2O_8^{2-} + Fe^{3+} \rightarrow Fe^{2+} + S_2O_8^{\bullet-} \tag{2}$$

$$SO_4^{\bullet-} + SO_4^{\bullet-} \rightarrow 2SO_4^{2-} \quad (k = 4.0 \times 10^8 M^{-1}s^{-1}) \tag{3}$$

$$SO_4^{\bullet-} + Fe^{2+} \rightarrow Fe^{3+} + SO_4^{2-} \quad (k = 4.6 \times 10^9 M^{-1}s^{-1}) \tag{4}$$

$$SO_4^{\bullet-} + S_2O_8^{2-} \rightarrow S_2O_8^{\bullet-} + SO_4^{2-} \quad (k = 6.1 \times 10^5 M^{-1}s^{-1}) \tag{5}$$

$$SO_4^{\bullet-} + H_2O \rightarrow SO_4^{2-} + H^+ + HO^{\bullet} (k_{[H_2O]} < 2.0 \times 10^{-3}s^{-1}) \tag{6}$$

PS concentration and Fe^{2+} concentration

Some articles (Liu *et al.* 2012; Long *et al.* 2014; Rao *et al.* 2014; Bu *et al.* 2016, 2017; Nie *et al.* 2018; Song *et al.* 2019; Wang *et al.* 2019c) investigated whether PS alone or Fe^{2+} alone can remove organics at room temperature. Some results (Bu *et al.* 2016, 2017; Nie *et al.* 2018; Wang *et al.* 2019c) showed that neither PS alone nor Fe^{2+} alone can remove organics under normal conditions. However, other results (Liu *et al.* 2012; Long *et al.* 2014; Rao *et al.* 2014; Song *et al.* 2019) presented that PS can remove 8–15% of organics. One of the possible causes is direct electron transfer oxidation from PS anion to organics, and another possible cause is the photocatalysis of light or temperature towards PS (Liu *et al.* 2012). Long *et al.* (2014) found that around 10% of organics were degraded due to the presence of Fe^{2+} alone. The principal reason has been proposed, a series of reactions (Equations (7)–(9)) under aerobic conditions eventually lead to the generation of $HO^{\bullet}$ that has the ability to degrade organics (Bu *et al.* 2016). This shows the high concentration of dissolved oxygen in the water can promote the degradation of organics by Fe^{2+} alone. Caré *et al.* (2013) demonstrated that Fe^{2+} is a reductant and in some cases can remove organics however if generated in-situ from iron powder, Fe^{2+} is more reactive since it is accompanied with the formation of additional iron corrosion products (ICPs) responsible for the co-precipitation and sequestration of organics along with reduction.

$$Fe^{2+} + O_2 \rightarrow Fe^{3+} + O_2^{-\bullet} \quad (\mathrm{pH} < 7, k < 10^{0.48}) \tag{7}$$

$$Fe^{2+} + O_2^{-\bullet} + 2H^+ \rightarrow Fe^{3+} + H_2O_2 \, (k = 1.0 \times 10^7) \tag{8}$$

$$Fe^{2+} + H_2O_2 \rightarrow Fe^{3+} + HO^{\bullet} + OH^- \, (k = 63 - 76) \tag{9}$$

PS and Fe^{2+} concentration in solution are critical parameters to generate $SO_4^{\bullet-}$, and the molar ratio of Fe^{2+} to PS also determines the $SO_4^{\bullet-}$ yield. Usually, the reaction to remove refractory organics is in two stages: at initial stage of reaction, the removal rate of organics increases with the increasing Fe^{2+} concentration or PS concentration; After initial stage, even the concentration of Fe^{2+} or PS continues to increase, the removal rate decreases. This shows that an appropriate molar ratio of Fe^{2+} to PS, rather than higher concentration of Fe^{2+} or PS, can obtain a better removal rate of organics. The most used molar ratio of Fe^{2+} to PS in these studies was 1:1, and followed by 1:2 according some literature (Oh *et al.* 2009; Liu *et al.* 2012; Bu *et al.* 2016; Wang & Wang 2017). From the reaction of Equation (1), we can see that, 1 mole of Fe^{2+} reacts with 1 mole of PS can produce 1 mole of $SO_4^{\bullet-}$. So, theoretically, 1:1 is

Table 2 | Reaction conditions and treatment effects in the Fe^{2+}/PS system

Pollutant (Abbreviation)	Parameters and degradation rate	Remarks	Reference
γ-hexachlorocyclohexane (γ-HCH)	[γ-HCH] = 0.0172 mM, [PS] = 42 mM, $[Fe^{2+}]$ = 0.0108 mM, pH = 5.7, t = 4 h, 100%	The γ-HCH oxidation rate constant (k) was relatively constant in the pH range of 3.5–9.0; however, it increased at both pHs 1.5 and 11.0.	Cao *et al.* (2008)
Polyvinyl alcohol (PVA)	$[Fe^{2+}]$:[PS] = 1:1, t = 120 min, T = 20 °C, 70%		Oh *et al.* (2009)
Orange G (OG)	[OG] = 0.1 mM, $[Fe^{2+}]$ = 1.0 mM, $[Fe^{2+}]$: [PS] = 1 : 4, pH = 3.5, t = 30 min, 81.0%	The following ions act as inhibitors are in sequence of NO_3^- <Cl^- <$H_2PO_4^-$ < HCO_3^-.	Xu & Li (2010)
Propachlor	[Propachlor] = 10 mg/ L, $[Fe^{2+}]$ = 2.5 mM, $[Fe^{2+}]$: [PS] = 1:2, pH = 4.0, T = 30 °C, t = 30 h, 60.0%	Neutral or even alkaline levels leaded to strong hydrolysis of Fe^{2+}, which had a negative effect on persulfate activation.	Liu *et al.* (2012)
Acetaminophen (APAP)	180 min, 18%	Sodium citrate at an appropriate concentration could improve the APAP degradation.	Deng *et al.* (2014)
Orange G (OG)	[OG] = 1.25 mM, $[Fe^{2+}]$: [PS] : [OG] = 10 : 20 : 5, pH = 3.0, T = 25 °C, t = 150 min, 35.0%		Han *et al.* (2014)
Toluene	[Toluene] = 1 mM, $[Fe^{2+}]$ = 5 mM, $[Fe^{2+}]$: [PS] = 1:4, pH = 7.0, t = 60 min, 70.0%	Excessive dosages of PS and Fe^{2+} inhibited toluene degradation efficiency; the optimal pH was 4.0.	Long *et al.* (2014)
Carbamazepine (CBZ)	[CBZ] = 0.025 mM, $[Fe^{2+}]$: [PS] : [CBZ] = 10:40:1, pH = 3.0, t = 40 min, 78.0%	The optimal pH was 4.22; NO_3^-, SO_4^{2-} and $H_2PO_4^-$ inhibited CBZ degradation rate, and Cl^- facilitated the decomposition of CBZ.	Rao *et al.* (2014)
1,4-dioxane (1,4-D)	[1,4-D] = 100 mg/L, $[Fe^{2+}]$ = 1,000 mg/L, $[Fe^{2+}]$: [PS] = 1 : 5, pH = 2.81, T = 40 °C, t = 51 h, 100%	The elevated temperature (50 °C and 60 °C) caused a slight decrease in the degradation rate of 1, 4-D with the addition of Fe^{2+}.	Zhao *et al.* (2014)
Levofloxacin (LFX)	[LFX] = 0.075 mM, $[Fe^{2+}]$: [PS] : [LFX] = 1 : 10 : 1, pH = 3.0, t = 1 min, 69.0%		Epold *et al.* (2015)
Chloramphenicol (CAP)	The effluent of a beef cattle operation [CAP] = 0.05 mM,[PS] = 1 mM, pH = 5.4,$[Fe^{2+}]$ = 0.1 mM,20 injections, t = 45 min, 90.1%	HCO_3^-, NO_3^-, NO_2^-, $H_2PO_4^-$, HPO_4^{2-} and HA demonstrates an adverse effect on CAP oxidation. Adding a low Cl^- concentration into solution can facilitate CAP degradation, but adding a high Cl^- concentration can inhibit CAP degradation.	Nie *et al.* (2015)
Reactive Black (RB5)	[RB5] = 0.01 mM, $[Fe^{2+}]$ = 8 mM, $[Fe^{2+}]$: [PS] = 1:50, pH = 7.78, t = 4 h, 98.0%	The higher initial concentration of RB5, the lower decolorization efficiency; the degradation rate of RB5 decreased with increasing pH; Cl^- could inhibit the degradation rate of RB5.	Satapanajaru *et al.* (2015)
Atrazine (ATZ)	[ATZ] = 20 μM, $[Fe^{2+}]$ = 0.4 mM, $[Fe^{2+}]$: [PS] = 1:1, t = 10 min, 57.0%	Low initial ATZ concentration was favorable for ATZ degradation rate.	Bu *et al.* (2016)
Ranitidine (RAN)	[PS] = 100 μM,$[Fe^{2+}]$ = 100 μM, [RAN] = 28.5 μM, pH = 6.45, T = 25 °C, t = 60 min, 96%	Under sequential spiking of Fe^{2+}, higher degradation efficiency 96% of RAN is obtained.	Naim & Ghauch (2016)
Atrazine (ATZ)	[ATZ] = 10 μM, $[Fe^{2+}]$ = 0.03 mM, [PS] = 1.0 mM, pH = 4.0, t = 15 min, 29.4%		Bu *et al.* (2017)

(*continued*)

Table 2 | continued

Pollutant (Abbreviation)	Parameters and degradation rate	Remarks	Reference
Amicarbazone (AMZ)	[AMZ] = 0.0414 mM, [Fe^{2+}] = 0.134 mM, [PS] = 2.5 mM, pH = 3.0, t = 60 min, 35.0%		Graça *et al.* (2017)
Sulfamethoxazole (SMX)	[SMX] = 0.05 mM, [PS] = 4 M, [Fe^{2+}]:[PS] = 1:1, T = 25 °C, t = 120 min, pH = 3.0, 100%	The actual composition of wastewater inhibited the degradation rate of SMX.	Wang & Wang (2017)
Ketoprofen (KTP)	[PS] = 0.5 mM,[Fe^{2+}] = 0.1 mM, [KTP] = 7.87 μM, pH = 6.15, T = 25 °C, t = 60 min, 98%	The optimal [Fe^{2+}]: [PS] ratio is 5:1.	Amasha *et al.* (2018)
Crystal violet (CV)	[CV] = 40 mg/L, [Fe^{2+}] = 0.3 mM, [Fe^{2+}]: [PS] = 3:4, pH = 7.0, t = 90 min, 41.0%	The optimal initial pH for degradation CV was 7.0.	Chen *et al.* (2018)
Bisphenol A (BPA)	[BPA] = 0.0877 mM, [PS] = 4.385 mM, [Fe^{2+}] = 0.0877 mM–0.877 mM, pH = 7.0, T = 25 °C, t = 60 min, 83.55% – 99.70%	A small amount of sodium citrate in the Fe^{2+}/PS system can lead to significant promotion of BPA removal in the rapid phase, and restore Fe^{3+} to Fe^{2+} to provide sustained activator for the slow phase. However, excessive sodium citrate can also inhibit the degradation.	Gao *et al.* (2018)
Chloramphenicol (CAP)	[CAP] = 0.05 mM, [Fe^{2+}] = 0.2 mM, [Fe^{2+}] : [PS] = 2:3, pH = 3.0, t = 100 min, 27.2%	Lower concentration of Cl^- (0.6–6 mM) slightly increased the CAP degradation rate, while higher Cl^- (12–36 mM) concentration inhibited CAP removal.	Nie *et al.* (2018)
Chlortetracycline (CTC)	[PS] = 500 mM, [Fe^{2+}] = 1,000 mM, [CTC] = 1 mM,t = 2 h, 76%	All Fe^{2+} ions in the case of homogeneous reaction activated above 90% PS to produce $SO_4^{\cdot-}$ which seems to be not efficient in degrading CTC due to scavenging of sulfate radicals by itself and also by excess Fe^{2+} ions.	Pulicharla *et al.* (2018)
Trimethoprim (TMP)	[TMP] = 0.05 mM, [PS] = 4 mM, [Fe^{2+}]:[PS] = 1:1, pH = 3.0, T = 25 °C, t = 250 min, 73.4%	The increasing persulfate concentration accelerated the TMP degradation rate; Under the same reaction conditions, the degradation rate of TMP in actual wastewater is 43.6%.	Wang & Wang (2018)
Acetaminophen (APAP)	[APAP] = 100 mg/L,pH = 6.5, [PS] = 0.8 g/L, [Fe^{2+}] = 0.7 mM, 90 min, 79%		Zhang *et al.* (2018c)
2,4,6-tricholoroanisole (TCA)	[PS] = 0.24 mM, [Fe^{2+}] = 0.48 mM, [TCA] = 0.47 μM, pH = 3, T = 20 °C, t = 60 min, 88%	The degradation of TCA by Fe^{3+}/PS was effective at both acidic and neutral pH comparing with alkaline pH.	Zhang *et al.* (2018b)
Diatrizoate (DTZ)	[DTZ] = 5 mg/L, [Fe^{2+}] = 1.0 mM, [Fe^{2+}] : [PS] = 1:10, pH = 3.0, T = 25 °C, t = 120 min, 69.0%	The degradation rate of DTZ increased only 3% when pH increased from 3.0 to 9.0, but DTZ degradation rate decreased significantly at pH 11.0; more than 99% of DTZ removal is acquired at 40 °C.	Shang *et al.* (2019)
Triphenyl phosphate (TPHP)	[TPHP] = 10 μM, [Fe^{2+}] = 1,000 μM, [Fe^{2+}]:[PS] = 2:1, pH = 4.0, T = 25 °C, t = 60 min, 80.0%	When pH increased from 4.0 to 9.0, removal rate TPHP was almost no changed.	Song *et al.* (2019)
Acetaminophen (ACT)	[ACT] = 0.05 mM, [Fe^{2+}] = 1 mM, [Fe^{2+}]:[PS] = 5:4, pH = 3.0, T = 20 °C, t = 40 min, 70.0%	Initial pH (3.0–9.0) had no insignificant impact on ACT degradation; ACT degradation rate decreased with initial ACT concentration increasing from 0.025 mM to 1 mM.	Wang *et al.* (2019c)

the optimal ratio of Fe^{2+} to PS. However, in fact, the optimal ratio can be greater than or less than 1:1, due to the presence of some oxidized or reduced substances in the complex sewage that can consume Fe^{2+} or PS. For example, $SO_4^{\bullet-}$ can react with excess Fe^{2+} or PS (Equations (4) and (5)) without considering the influence of other ions. In addition, the ratio of oxidant (PS) or catalyst (Fe^{2+}) concentration to organics concentration is also an important factor for maintaining a better organics removal rate. Some studies (Satapanajaru *et al.* 2015; Wu *et al.* 2015; Bu *et al.* 2016; Nie *et al.* 2018) stated that the concentration of oxidant or catalyst required is proportional to the concentration of contaminants due to more pollutants require more $SO_4^{\bullet-}$ generated from PS activated by Fe^{2+}.

Solution pH

The initial pH of aqueous solution is an important factor influencing the removal efficiency of refractory organics in Fe^{2+}/PS system. Some articles (Cao *et al.* 2008; Xu & Li 2010; Liu *et al.* 2012; Niu *et al.* 2012; Long *et al.* 2014; Rao *et al.* 2014; Epold *et al.* 2015; Han *et al.* 2015a; Satapanajaru *et al.* 2015; Wu *et al.* 2016; Nie *et al.* 2018; Yu *et al.* 2018; Shang *et al.* 2019; Song *et al.* 2019; Wang *et al.* 2019c) studied the effect of pH ranging from 2.0 to 11.0 on the removal of refractory organics in Fe^{2+}/PS system. Based on the results of these articles (Xu & Li 2010; Liu *et al.* 2012; Niu *et al.* 2012; Long *et al.* 2014; Rao *et al.* 2014; Han *et al.* 2015a; Satapanajaru *et al.* 2015; Wu *et al.* 2016; Nie *et al.* 2018), the optimum pH range was 3.0–4.0. Within such a pH range, due to acid catalysis on PS, more $SO_4^{\bullet-}$ could be generated from decomposition of PS, which therefore enhanced the removal rate of organics (Nie *et al.* 2018). When the pH was less than 3.0, refractory organics removal rate decreased because pH < 3.0 promotes the formation of the ferrous complex $(Fe(H_2O))^{2+}$, which reduces the amount of Fe^{2+} to activate PS, and thus less $SO_4^{\bullet-}$ can be formed. When the initial pH increased from 4.0 to 9.0, the removal efficiency of refractory organics gradually decreased. Four mechanisms are summarized to explain the reason why refractory organics degradation declined with increasing pH:

(1) When the pH is higher than 4.0, free Fe^{2+} turns into Fe^{2+} complexes (Equation (10)), which inhibits the further reaction between Fe^{2+} and PS to form $SO_4^{\bullet-}$ (Xu & Li 2010; Rao *et al.* 2014; Nie *et al.* 2018).

$$Fe^{2+} + H_2O \rightarrow FeOH^{+} + H^{+} \ (k = 1.9s^{-1}) \quad (10)$$

(2) With pH increasing above 4.0, ferric hydroxide complexes, such as $FeOH^{2+}$, $Fe_2(OH)_2^{4+}$, $Fe(OH)^{2+}$, $Fe(OH)_3$, and $Fe(OH)_4^-$ formed in the solution have low activation capacity to generate $SO_4^{\bullet-}$ from PS, thus the efficiency of the refractory organics degradation is reduced (Nie *et al.* 2018). The equations of generating ferric hydroxide complexes are shown in Equations (11)–(13) (Xu & Li 2010). It can be seen from these equations that hydrogen ion is generated during the reaction and causes the decrease of pH in the solution.

$$Fe^{3+} + H_2O \rightarrow FeOH^{2+} + H^{+} \ (k = 2.3 \times 10^{7}s^{-1}) \quad (11)$$

$$Fe^{3+} + 2H_2O \rightarrow Fe(OH)^{2+} + 2H^{+} \ (k = 4.7 \times 10^{3}s^{-1}) \quad (12)$$

$$2Fe^{3+} + 2H_2O \rightarrow Fe_2(OH)_2^{4+} + 2H^{+} (k = 1.1 \times 10^{7}s^{-1}) \quad (13)$$

(3) If the pH is higher than 8.5, the present PS in the solution may react with OH^- to form $OH^{\bullet}$ (Equation (14)) in alkaline solution (Satapanajaru *et al.* 2015). This results in the rapid decay of $SO_4^{\bullet-}$ (Liu *et al.* 2012; Satapanajaru *et al.* 2015). But hydroxyl radical is also strong in its reaction with the organic compounds.

$$SO_4^{-\bullet} + OH^- \rightarrow SO_4^{2-} + {}^{\bullet}OH \quad (14)$$

(4) When the pH is greater than or equal to 8.4, $SO_4^{\bullet-}$ was found to react with HCO_3^- or CO_3^{2-} (Equations (15) and (16)) to form $HCO_3^{\bullet}$ or $CO_3^{\bullet}$, any of which has poor oxidizing ability toward organics compared to $SO_4^{\bullet-}$ (Satapanajaru *et al.* 2015).

$$SO_4^{-\bullet} + HCO_3^- \rightarrow SO_4^{2-} + HCO_3^{\bullet} \quad \text{at pH} = 8.4 \quad (15)$$

$$SO_4^{-\bullet} + CO_3^{2-} \rightarrow SO_4^{2-} + CO_3^{\bullet} \quad \text{at pH} > 8.4 \quad (16)$$

Several articles (Epold *et al.* 2015; Shang *et al.* 2019; Song *et al.* 2019; Wang *et al.* 2019c) claimed that an initial solution pH (3.0–7.0) has no significant effect on removing refractory organics. Wang *et al* (2019c) investigated the degradation of acetaminophen (ACT) in the Fe^{2+}/PS system at different initial pH (3.0, 5.0, 7.0 and 9.0), and found that the degradation of ACT was around 70% after a 30-min reaction at each of initial solution pH. In the article by Wang *et al.* (2019c), regardless of how the initial pH changed (from 3.0 to 9.0), the pH of the solution after 1-min reaction dropped

rapidly to 3.0, which demonstrates the degradation of ACT was not affected by the initial pH in Fe^{2+}/PS system. Song *et al.* (2019) studied the effect of increasing pH from 4.0 to 9.0 on the degradation efficiency of triphenyl phosphate (TPhP) in Fe^{2+}/PS process and found that degradation efficiency of TPhP was not impacted by pH changes. Epold *et al.* (2015) investigated levofloxacin (LFX) degradation at different pH (3.0, 5.0, 7.0 and 9.0) in Fe^{2+}/PS system, and the degradation rates of LFX acquired were almost as same as pH from 3.0 to 7.0, while the degradation rate of LFX was decreased by about 10% at pH of 9.0. Shang *et al.* (2019) studied the influence of initial pH (3.0, 5.0, 7.0, 9.0 and 11.0) on diatrizoate (DTZ) degradation. It was found that DTZ degradation rate was increased to only 3% when the pH was increased from 3.0 to 9.0. However, DTZ degradation efficiency dropped significantly as the initial pH increased from 9.0 to 11.0. Shang *et al.* (2019) proposed that the decreased DTZ degradation at initial pH of 11.0 is due to the reduction of Fe^{2+} that tended to be hydrolyzed to ferric hydroxide and ferrous hydroxide under alkali conditions.

The findings of Cao *et al.* (2008) were different from the above articles. They testified that both low (pH = 1.5) and high pH (pH = 11.0) were more favorable for oxidation of Lindane in Fe^{2+}/PS system. The proposed reason is that Lindane is easily catalyzed hydrolysis by acid or base.

Anions concentration

Some inorganic anions, such as HCO_3^-, NO_3^-, NO_2^-, SO_4^{2-}, $H_2PO_4^-$ and Cl^-, in the water either have a positive or negative effect on sulfate radicals-based oxidation. This inorganic anion can either promote or inhibit the degradation of refractory organics in the Fe^{2+}/PS system. The conclusions from some articles (Xu & Li 2010; Ghauch *et al.* 2013; Rao *et al.* 2014; Naim & Ghauch 2016; Bu *et al.* 2017; Amasha *et al.* 2018; Nie *et al.* 2018; Song *et al.* 2019; Wang *et al.* 2019c) indicated that NO_3^-, SO_4^{2-}, $H_2PO_4^-$ and HPO_4^{2-} could inhibit degradation of refractory organics, while Cl^-, HCO_3^- could play both positive and negative effects on refractory organics removal. The inhibition effect of NO_3^-, SO_4^{2-}, $H_2PO_4^-$, HCO_3^- and Cl^- is attributed to the reactions occurring between inorganic anions and $SO_4^{\bullet-}$ (Equations (17)–(20)). $H_2PO_4^-$, NO_3^-, Cl^- and HCO_3^- could react with $SO_4^{\bullet-}$, then generate $HPO_4^{\bullet-}$, $NO_3^{\bullet}$, $Cl^{\bullet}$ and $CO_3^{\bullet2-}$, respectively. Because the redox potential of $HPO_4^{\bullet-}$, $NO_3^{\bullet}$, $Cl^{\bullet}$ and $CO_3^{\bullet2-}$ are lower than that of $SO_4^{\bullet-}$, the replacement of these free radicals with $SO_4^{\bullet-}$ leads to a decrease in the rate of degradation of refractory organics in Fe^{2+}/PS system. Phosphate is a special case in PS systems activated by iron species. In fact phosphate is a good complexant for Fe^{2+} species to form $FeH_2PO_4^{2+}$ and $FePO_4$ (Ghauch 2008) and this is why inhibition occurs. Unless done in Fe^{2+} free solution, phosphate can generate in heat activated PS medium some phosphate radicals as mentioned here (Ghauch & Tuqan 2012).

As for the effect of SO_4^{2-} on refractory organics removal, the possible reason is due to the high ion strength that hinders the decomposition of PS (Rao *et al.* 2014). In addition, SO_4^{2-} can reduce the reduction potential of half reaction of $SO_4^{\bullet-}$ ($E^{\theta}_{(SO_4^{\bullet-}/SO_4^{2-})}$), which also results in the reducing ability of $SO_4^{\bullet-}$ oxidation on refractory organics (Rao *et al.* 2014). One proposal for the positive effect of Cl^- on the organics degradation is that the formation of chlorine-containing radicals ($Cl^{\bullet}$ and $Cl_2^{\bullet-}$) and free available chlorine (Cl_2) through a series of chain reactions (Equations (21)–(24)) enhances the refractory organics removal (Rao *et al.* 2014; Wang *et al.* 2019c). Among these free radicals, $Cl_2^{\bullet-}$ as a stronger oxidizing property is major free radical when the Cl^- concentration reached 10.0 mM (Wang *et al.* 2019c). From the research of Song *et al.*, 100 mM HCO_3^- enhanced TPhP degradation to 66.6% in Fe^{2+}/PS process (Song *et al.* 2019). There are two possible reasons to explain the promotion of TPhP degradation by carbonate (Song *et al.* 2019). Firstly, HCO_3^- can easily react with electron-rich organic pollutants like TPhP. Alternatively, high concentration of HCO_3^- can stimulate the decomposition of PS into $SO_4^{\bullet-}$, and promote the TPhP removal.

$$H_2PO_4^- + SO_4^{\bullet-} \rightarrow HPO_4^{\bullet-} + HSO_4^- \ (k = 6.0 \times 10^4 M^{-1}s^{-1}) \quad (17)$$

$$NO_3^- + SO_4^{\bullet-} \rightarrow NO_3^{\bullet-} + SO_4^{2-} \ (k = 3.6 \times 10^5 M^{-1}s^{-1}) \quad (18)$$

$$Cl^- + SO_4^{\bullet-} \rightarrow Cl^{\bullet-} + SO_4^{2-} \ (k = 4.7 \times 10^8 M^{-1}s^{-1}) \quad (19)$$

$$HCO_3^- + SO_4^{\bullet-} \rightarrow CO_3^{\bullet2-} + H^+ + SO_4^{2-} \ (k = 2.8 \times 10^6 M^{-1}s^{-1}) \quad (20)$$

$$SO_4^{\bullet-} + Cl^- \rightarrow Cl^{\bullet} + SO_4^{2-} \quad (21)$$

$$Cl^{\bullet} + Cl^- \rightarrow Cl_2^{\bullet-} \quad (22)$$

$$Cl_2^{\bullet-} + Cl_2^{\bullet-} \rightarrow Cl_2 + 2Cl^- \quad (23)$$

$$Cl^{\bullet} + Cl^{\bullet} \rightarrow Cl_2 \quad (24)$$

Chelating agents

Because too much or too little Fe^{2+} in solution has an adverse effect on activating PS to generate $SO_4^{\bullet-}$, the chelating agents were used in Fe^{2+}/PS system to avoid the drawback of alone utilization of Fe^{2+}. Various chelating agents were added to aqueous solution in the form of acids or salts to chelate with Fe^{2+}, such as hydroxylamine (HA), citric acid (CA), oxalic acid (OA), tartaric acid (TA), ethylenediaminetetraacetate (EDTA), (S,S) – ethylenediamine – N, N′ – disuccinate (EDDS), sodium thiosulfate ($Na_2S_2O_3$), diethylene triamine pentaacetic acid (DTPA) and epigallocatechin-3-gallate (EGCG) (Zhou *et al.* 2013; Han *et al.* 2014, 2015a; Ji *et al.* 2014; Wu *et al.* 2015, 2016; Bu *et al.* 2017; Yu *et al.* 2018). Han *et al.* (2014), Wu *et al.* (2015) and Wu *et al.* (2016) concluded that HA is an effective chelating agent that could alleviate Fe^{3+} accumulation and accelerate Fe^{2+} regeneration (Equations (25)–(27)); the results shows an addition of HA can promote refractory organics removal rate.

$$Fe^{3+} + NH_2OH \rightarrow NH_2O^{\bullet} + Fe^{2+} + H^+ \quad (25)$$

$$Fe^{3+} + NH_2O^{\bullet} \rightarrow NHO + Fe^{2+} + H^+ \quad (26)$$

$$5Fe^{3+} + 2H_2O + NH_2O^{\bullet} \rightarrow NO_3^- + 5Fe^{2+} + 6H^+ \quad (27)$$

In the article by Ji *et al.* (2014), three kinds of chelating agents, CA, EDTA, and EDDS, were used to assist Fe^{2+} in activating PS. The study of their effects on antibiotics degradation indicates that CA and EDTA both have some promoting effect on sulfamethoxazole (SMX) degradation, while CA, EDTA, and EDDS did not show a significant impact on ciprofloxacin (CIP) degradation, which means that the effects of the chelating agents varies from different targeted contaminants. The article by Zhou *et al.* (2013) testified the addition of $Na_2S_2O_3$ could facilitate the removal of diuron by about 25% compared with no $Na_2S_2O_3$ added under the same conditions. This was due to $Na_2S_2O_3$, acting as a buffer, balancing the amount of Fe^{3+} and Fe^{2+}, as Equations (28)–(30).

$$XS_2O_3^{2-} + YFe^{2+} \rightarrow Complexanion \quad (28)$$

$$Complexanion + S_2O_8^{2-} \rightarrow Fe^{3+} + SO_4^{\bullet-} + SO_4^{2-} + residue \quad (29)$$

$$S_2O_3^{2-} + Fe^{3+} \rightarrow Fe^{2+} + 1/2S_4O_6^{2-} \quad (30)$$

EGCG as green tea extract, was tested by Bu *et al.* (2017), and the result showed that EGCG could enhance the degradation rate of atrazine from 70% to 100% between pH 2.0 and 7.0. Owing to the strong chelating and reducing ability of EGCG, it accelerated the transformation rate from Fe^{3+} to Fe^{2+}, as showed in Equations (31)–(33) (Bu *et al.* 2017).

$$Fe^{3+} + EGCG \rightarrow [Fe(EGCG)]^+ + 2H^+ \quad (31)$$

$$[Fe_2(EGCG)]^{2+} \rightarrow Semiquinone\ type\ product \quad (32)$$

$$Semiquinone\ type\ product + 2Fe^{3+} \rightarrow Benzoquinone\ type\ product + 2Fe^{2+} \quad (33)$$

From the above research results on chelating agents, we know that some chelating agents can promote the efficiency of Fe^{2+} activation reaction under certain conditions in the Fe^{2+}/PS process, and these reaction conditions need to be further explored. In another point, the chelating agents used in the Fe^{2+}/PS system should be considered not to cause secondary pollution to the solution and to be easily biodegraded.

ZERO-VALENT IRON-RELATED ACTIVATORS

Zero-valent iron (Fe^0)

Although Fe^{2+} appears to be a good activator for PS, Fe^{2+}/PS systems still have some limitations such as scavenging effect of excess Fe^{2+} on $SO_4^{\bullet-}$, conversion of Fe^{2+} to iron hydroxide precipitation, and acidic pH of the solution. Fe^0 has been widely studied as an alternative source of Fe^{2+} because it can gradually release ferrous iron into the water.

In a Fe^0/PS system, Fe^0 is corroded under aerobic (Equation (34)) or anaerobic (Equation (35)) conditions to form Fe^{2+}; the formed Fe^{2+} further reacts with PS to generate $SO_4^{\bullet-}$, which is consistent with Equation (1). Moreover, based on Equation (36), $SO_4^{\bullet-}$ could be generated straight through electron transformation from Fe^0 to $S_2O_8^{2-}$. According to Equation (37), the recycling of Fe^{2+} on the surface of Fe^0 can effectively avoid the accumulation of excess Fe^{2+} so that the amount of iron hydroxide reproduction can be reduced in the Fe^0/PS system.

$$2Fe^0 + O_2 + 2H_2O \rightarrow 2Fe^{2+} + 4OH^- \quad (34)$$

$$Fe^0 + 2H_2O \rightarrow Fe^{2+} + 2OH^- + H_2 \quad (35)$$

$$Fe^0 + S_2O_8^{2-} \rightarrow Fe^{2+} + 2SO_4^{2-} + 2SO_4^{\bullet-} \quad (36)$$

$$Fe^0 + 2Fe^{3+} \rightarrow 3Fe^{2+} \quad (37)$$

Table 3 summarizes the reaction conditions and degradation efficiency of some refractory organics using Fe^0 as

Table 3 | Reaction conditions and EC treatment effects in the Fe^0/ PS system

Pollutant (Abbreviation)	Parameters and degradation rate	Remarks	Reference
Polyvinyl alcohol (PVA)	$[Fe^0]/[PS] = 1:1$,120 min, T = 20 °C, [PS] = 250 mg/L, PVA = 47.1–50.2 mg/L, 100%	The optimal persulfate to Fe^{2+} or Fe^0 molar ratio was found to be 1:1.	Oh *et al.* (2009)
Naphthalene (NAP)	[NAP] = 10 mg/L, [PS] = 42 mM, $[Fe^0]$ = 1 g/L, T = 20 °C,pH = 5.0, 3 min, 99%	The initial pH of 5.0 changed to around 2.3 in the NAP/PS/Fe^0 systems after reaction.	Liang & Guo (2010)
2,4-dinitrotoluene (DNT)	[PS] = 250 mg/L, $[Fe^0]$ = 1 g/L, [DNT] = 50 mg/L, t = 300 min, 91%	As a persulfate-activating agent, Fe^0 is more effective and longer-lasting than Fe^{2+} and potentially more suitable for environmental applications.	Oh *et al.* (2010)
4-chlorophenol	$[Fe^0]$ = 0.20 g/L, [4-chlorophenol] = 0.156 mM; [PS] = 0.78 mM, no pH adjustment, t = 1 h, 88%	The removal of 4-chlorophenol with Fe^0-PS was 86% and 80% at pH 3.0 and 6.0, respectively.	Zhao *et al.* (2010)
p-chloroaniline (PCA)	[PCA] = 0.05 mM, [PS] = 2.5 mM, $[Fe^0]$ = 0.70 g/L, pH = 6.8, t = 300 min, 64.55%	The PCA degradation was higher under acidic conditions (pH 2.0 and 4.0) compared to alkaline conditions. Complete degradation of PCA was obtained by ZVI-activated persulfate at pH 4.0 at 12 min.	Hussain *et al.* (2012)
Sulfamethoxazole (SMX)	$[Fe^0]$ = 17.85 mM, [PS] = 1.0 mM, [SMX] = 39.5 ìM, pH = 5.54, t = 2 h, 91%	Reactions with acid-washed MIPs (wFe/SMX) were more successful than those carried out with un-washed MIPs (nwFe/SMX).	Ghauch *et al.* (2013)
Acetaminophen (APAP)	$[Fe^0]$:[PS] = 1:1,180 min, 93.19%	The Fe^0/PS system was effective in a broader pH range from 3.0 to 8.5; heat could enhance the APAP degradation.	Deng *et al.* (2014)
Aniline	$[Fe^0]$ = 0.4 g/L, [Aniline] = 0.05 mM, T = 25 °C, [PS] = 2.5 mM, pH = 7.0, t = 300 min, 85%	The optimum pH for degradation of aniline was 4.0 in which 100% degradation efficiency was achieved after 10 min reaction.	Hussain *et al.* (2014)
Dibutyl phthalate (DBP)	[DBP] = 5 mg/L; [PS] = 43 mg/L; $[Fe^0]$ = 0.3 g/L; T = 25 C, pH = 3.0, t = 120 min, 84%	The half-lives for the oxidation of DBP in Fe^0/PS were 30–176 min at pH 3.0–11.0.	Li *et al.* (2014)
Acid Orange 7 (AO7)	[AO7] = 30 mg/L,[PS] = 0.3 g/L, $[Fe^0]$ = 0.5 g/L, pH = 5.8,20 min, 38%		Wang *et al.* (2014)
Sulfadiazine (SD)	[SD] = 20 mg/L, [PS] = 1.84 mM, $[Fe^0]$ = 0.92 mM, pH = 7.0, t = 1 h, 45.5%		Zou *et al.* (2014)
1,1,1-trichloroethane (TCA)	[PS] = 9.0 mM, [TCA] = 0.15 mM, $[Fe^0]$ = 2.08 g/L, T = 25 °C, t = 6 h, 90%	There was no significant difference on degradation efficiency of TCA under pH 6–8.	Gu *et al.* (2015)
Acid orange 7 (AO7)	[PS]:[AO7] = 30:1, [AO7] = 0.2 mM, $[Fe^0]$ = 0.5 g /L, pH = 3.8, T = 25 °C, 10 min, 88% AO7 removal	The overall oxidation rate of AO7 was inhibited upon addition of NO_3^-, NO_2^-, SO_4^{2-}, Cl^-, CO_3^{2-}, HCO_3^-, HPO_4^{2-}, $H_2PO_4^-$ and EDTA, whereas ClO_4^-, CH_3COO^- and HA were found to accelerate AO7 decolorization rates.	Li *et al.* (2015)
Chloramphenicol (CAP)	[CAP] = 0.05 mM, $[Fe^0]$ = 1 mM, [PS] = 1 mM, pH = 5.4,50 min, 95%	The optimum molar ratio of CAP/ZVI/PS is 1:20:20.	Nie *et al.* (2015)
Sirius Red F3B (SRF3B)	[SRF3B] = 25 mg/L, pH = 6.0, [PS] = 5 mM, $[Fe^0]$ = 0.5 g/L, 10 min, 95% decolorization 120 W/L US	The PS/(Fe^0) system shows a practically feasible process for SRF3B decolorization under conditions of initial pH <9.0, high PS and Fe^0 dosages, and high temperatures.	Weng *et al.* (2015)
Para-Chlorophenol (PCP)	[PS] = 15 mM, $[Fe^0]$ = 1 g/L, [PCP] = 50 mg/L, pH = 5.0, T = 25 °C, t = 120 min, 70%	The degradation efficiency of PCP gradually decreases to 51.7% when the ZVI reuse time is increased.	Ahmadpour & Yengejeh (2016)

(*continued*)

Table 3 | continued

Pollutant (Abbreviation)	Parameters and degradation rate	Remarks	Reference
Triton X – 45 (TX – 45)	[TX – 45] = 20 mg/L, [Fe^0] = 1 g/L, [PS] = 2.5 mM, pH = 5.0, t = 60 min, 90%	TX – 45 and TOC removals were most efficient under acidic and neutral pH valueswith addition of 2.5 mM PS.	Temiz *et al.* (2016)
Alachlor	[Alachlor] = 5 mg/L,[Fe^0] = 2.0 mM, [PS] = 1.0 mM, T = 30 °C, 60 min, 100%	The reaction rate is significantly influenced by factors such as Fe^0 dosage, PS dosage, initial pH, temperature, NOM, citrate and anions.	Wang *et al.* (2016b)
Direct Red 23 (DR23)	[DR23] = 0.1 mM, [PS] = 5 mM, [Fe^0] = 0.5 g/L, pH = 6,T = 25 °C, t = 15 min, 95%	A promising decolorization was observed in the PS oxidation process activated with Fe^0 aggregates. The decolorization efficiency in the PS/Fe^0 system was further enhanced by US (PS/Fe^0/US) or heat (PS/Fe^0/55 °C).	Weng & Tsai (2016)
Orange G (OG)	[OG] = 0.2 mM, [PS] = 2 mM, [Fe^0] = 0.2 g/L, CuO = 0.1 g/L,T = 25 °C, pH = 5.0, t = 1 h, 50%		Wang *et al.* (2016a)
Bentazon (BTZ)	[Fe^0] = 4.477 mM,[PS] = 0.262 mM, [BTZ] = 0.021 mM, pH ≤ 7, 100%	Al^{3+}, Cl^-, NO_3^- improved the treatment; NH_4^+, Ca^{2+}, and Mg^{2+} did not significantly influence the BTZ removal; and Mn^{2+}, Cu^{2+}, CO_3^{2-} HCO_3^-, PO_4^{3-}, HPO_4^{2-}, $H_2PO_4^-$ inhibited the BTZ degradation.	Wei *et al.* (2016)
Reactive Green 19 (RG19)	[RG19] = 0.01 mM, [PS] = 5 mM, [Fe^0] = 1.0 g/L, pH = 6.0, T = 25 °C, 10 min, 99% sodium citrate, sodium EDTA, and [sodium oxalate] = 1 mM	RG19 decolorization decreased from 99% to 7%, 21%, and 15% in presence of sodium citrate, sodium EDTA, and sodium oxalate, compared with control test (without chelating agent, 99%) within 10 min.	Ding *et al.* (2017)
p-nitrophenol (PNP)	[PNP] = 500 mg/L, [Fe^0] = 30 g/ L, [PS] = 12.5 mM, pH = 3.6, T = 25 °C, 3 min, 95%		Ji *et al.* (2017)
1,4-dioxane (1,4-D)	[Fe(0)]:[PS] = 1:1, [Fe^0] = 67 mM, [PS] = 63 mM,[PS] :[dioxane] = 11:1, t = 10 min, 60% of dioxane removal	Distributing the Fe^0 as eight, one-eighth dosages, 95% dioxane removal was achieved; adding sodium hexametaphosphate (SHMP) to the persulfate candles can facilitate persulfate release.	Kambhu *et al.* (2017)
p-nitrophenol (PNP)	[Fe^0] = 1.3 g/L, [PS] = 6.7 mM, pH = 5.1, 20 min, 29.6%		Li. *et al.* (2017a)
Erythromycin (ERY)	[Fe^0] = 22.4 mg L, [PS] = 0.1 mM; [ERY] = 1 mg L,T = 25 °C, initial pH, t = 240 min, 91.2%	The ERY removal was more favorable under acidic and neutral condition than alkaline condition.	Li *et al.* (2017b)
2,4-dichlorophenol (2,4-DCP)	[Fe^0] = 1.5 mM, [2,4-DCP] = 4 mg/L, [PS] = 1.0 mM, pH = 7,15 min, 90%	The Pre-Fe^0/PS system induced a significant improvement in removal efficiency of 2,4-DCP, TOC and de-chlorination, especially at a higher initial pH condition.	Li. *et al.* (2017c)
Orange G (OG)	[Fe^0] = 4 mM, [PS] = 4 mM, [OG] = 200 mg/ L, pH = 7, 180 min, 28.6%		Pan *et al.* (2017)
Sulfadiazine (SDZ)	[Fe^0] = 1 mM, [PS] = 1 mM, [SDZ] = 20 mM, T = 25 °C, pH = 7,10 min, 80%	Common aquatic materials including sulfate, nitrate, chloride, perchlorate, and HA all showed a negative effect on SDZ degradation by Fe^0/PS following a trend of Cl^- < ClO_4^- < SO_4^{2-} < NO_3^- <HCO_3^- < HA.	Yang & Che (2017)
Bisphenol A (BPA)	[BPA] = 0.0877 mM, [PS] = 4.385 mM, [Fe^0] = 0.0877 mM–0.877 mM pH = 7.0, T = 25 °C, t = 60 min, 85.17% – 100%	The best BPA decomposition effects were obtained when [Fe^{2+}]:[PS] = 1:2 and [Fe^0]: [PS] = 1:2 are applied.	Gao *et al.* (2018)

(*continued*)

Table 3 | continued

Pollutant (Abbreviation)	Parameters and degradation rate	Remarks	Reference
Chlortetracycline (CTC)	$[Fe^0] = 1{,}000$ mM, 94%	Whereas in heterogeneous reactions, slow generation and regeneration of Fe^{2+} ions obtained a removal of CTC above 90%.	Pulicharla *et al.* (2018)
Rhodamine B (RhB)	[RhB] = 50 mg/ L, [PS] = 1.4 g/L, H_2A/ Fe^0 = 1.0 g/ L, T = 25 °C, 60 min, 58%	The optimal PS dosage is 0.3 g/L.	Wang *et al.* (2018)
Remazol Golden Yellow (RGY)	[PS] = 5×10^{-3} M, $[Fe^0]$ = 0.5 g/L, [RGY] = 100 mg/L, pH = 6.0, t = 20 min, 98%	The inhibitory effect of various inorganic salts on decolorization follows the sequence of Na_2HPO_4> $NaHCO_3$ > $NaClO_4$ > NaCl > $NaNO_3$ > $NaClO_4$ > no salt.	Weng & Tao (2018)
2,4,6-tricholoroanisole (TCA)	[PS] = 0.24 mM, $[Fe^0]$ = 0.48 mM, pH = 7, [TCA] = 0.47ìM, temperature: T = 25 °C; t = 60 min, 18%	CA/Fe^0 molar ratio of 2:5, CA promoted the oxidation of TCA by Fe^0/PS, but OA and EDTA retarded the reaction. Citric acid(CA),oxalic acid(OA)Fe^0/PS had the best performance at pH 2.5.	Zhang *et al.* (2018b)

an activator for PS to generate $SO_4^{\bullet-}$. It can be seen from Table 3 that most of the activation reactions in Fe^0/PS system can achieve high refractory organics removal rates of 70–100% in the range of pH 3.0–7.0. Some papers (Oh *et al.* 2009; Deng *et al.* 2014; Pulicharla *et al.* 2018; Zhang *et al.* 2018b) compared the effects of Fe^0 and Fe^{2+} acting as activators for PS on refractory organics removal and all results showed that Fe^0 has a better treatment effect on refractory organics degradation than Fe^{2+} under the same conditions of the reaction. Except, the results of Gao *et al.* (2018) showed that Fe^0 and Fe^{2+} both had the same removal effect on bisphenol A removal at neutral pH. Under most conditions, the activation effect of Fe^0 on PS is still better than that of Fe^{2+} on PS. Similar to previously discussed Fe^{2+}/PS system, the molar ratio of catalyst to oxidant is an important parameter in Fe^0/PS system. Low Fe^0:PS molar ratio will lead to poor degradation effect on refractory organics due to lack of sufficient active sites for PS activation and $SO_4^{\bullet-}$ generation, while high Fe^0: PS molar ratio will result in less $SO_4^{\bullet-}$ production and unnecessary Fe^0 consumption. According to previous analysis, we know the theoretically optimal ratio of Fe^{2+}: PS was 1:1. However, Fe^0: PS molar ratio needs to be higher than 1:1 in the bulk solution in order to ensure enough Fe^0 that can consistently liberate Fe^{2+} into the water. Moreover, the ratio of catalyst to oxidant ultimately should be determined under specific reaction conditions.

Fe^0 shows a good activated effect on PS. However, high concentrations of Fe^0 and PS are required, which increases treatment cost. In order to improve efficiency of Fe^0 on PS decomposition, researchers used two thin cylindrical neodymium-iron-boron permanent magnets to make Fe^0 magnetic, and magnetized Fe^0 (or pre-magnetization Fe^0) was employed to activate PS for degrading refractory organics, such as orange (OG), 2,4-dichlorophenol (2,4-DCP) (Li *et al.* 2017c; Pan *et al.* 2017). It was found that in SEM micrographs, after pre-magnetization, the Fe^0 surface was slightly corroded and deposition of tiny particles it was noted on the surface and the BET after pre-magnetization significantly increased from 0.15 m^2/g (original Fe^0) to 1.94 m^2/g, which benefited the mass transfer of Fe^{2+} released from Fe^0 (Li *et al.* 2017c). For these reasons, the degradation rate of refractory organics in the pre-magnetized Fe^0/PS is also higher than Fe^0/PS system (Li *et al.* 2017c; Pan *et al.* 2017).

Nano-sized zero-valent iron

To further improve the efficiency of Fe^0/PS system, nFe^0 has been used to activate PS for refractory organics removal because of high activity of nFe^0 compared with Fe^0. Better refractory organics removal efficiency has been found in nFe^0/PS system than Fe^{2+}/PS or Fe^0/PS (Al-Shamsi & Thomson 2013; Zhu *et al.* 2016; Wang *et al.* 2017; Kim *et al.* 2018; Lin & Chen 2018). Lin & Chen (2018) used nFe^0 for PS decomposition to degrade sulfamethazine (SMT), and the SMT removal rate of 93% was obtained in 5 min with addition of nFe^0 of 56 mg/L and PS of 2 mM. Al-Shamsi & Thomson (2013) compared the degradation rate of TCE using three different iron activators of nFe^0, Fe^0 and Fe^{2+}. The TCE degradation rate in 3 min by nFe^0/PS was 1.11×10^{-4} Mmin^{-1}, which is higher than that of Fe^0/PS (5.18×10^{-6} Mmin^{-1}) and Fe^{2+}/PS

(6.25×10^{-5} Mmin^{-1}). Zhu *et al.* (2016) also studied the effects of the three iron activators for DDT removal, and the result is similar to Wang *et al.* (2017). To sum up, it is proposed that more $SO_4^{\cdot-}$ were formed in nFe^0/PS than Fe^{2+}/PS or Fe^0/PS because of large specific surface areas of nFe^0. Although valence of the Fe^0 and nFe^0 is same, nFe^0 has a different surface structure from Fe^0. Generally, there is formed a cycle of Fe^{3+} and Fe^{2+} on the surface of Fe^0. Al-Shamsi & Thomson (2013) used X-ray photoelectron spectroscopy analyzed the surface of nFe^0; they found that there was a layer of FeOOH (ferric oxyhydroxideon) on the surface of fresh nFe^0. Furthermore, a passivated iron sulfate layer was formed on the nFe^0 surfaces as fresh nFe^0 contacts with the PS. The mechanism of the FeOOH layer formation are presented on Equations (34)–(41).

$$Fe^{2+} + H_2O \rightarrow Fe^{3+} + OH^- + 1/2H_2 \quad (38)$$

$$Fe^{3+}_{(ads)} + 3OH^- \rightarrow Fe(OH)_{3(s)} \quad (39)$$

$$Fe^{3+}_{(ads)} + 3H_2O \rightarrow Fe(OH)_{3(s)} + 3H^+ \quad (40)$$

$$Fe(OH)_{3(s)} \rightarrow FeOOH_{(s)} + H_2O \quad (41)$$

The mechanism of formation of ferrous sulfate layer can be explained by some equations. The reaction between nFe^0 and PS is as same as Fe^0 and PS, and the products of the reactions in Fe^0/PS system and Fe^{2+}/PS system both include $SO_4^{\cdot-}$ and SO_4^{2-} (Equation (36)). Some Fe^{2+} react with PS to form SO_4^{2-} (Equation (1)), some Fe^{2+} scavenge $SO_4^{\cdot-}$ to generate SO_4^{2-} (Equation (2)). Surplus SO_4^{2-} can react with Fe^0 or FeOOH to produce ferrous sulfate precipitated on the surface of nFe^0 (Equations (42) and (43)). Although the layer of ferrous sulfate on the nFe^0 surface will reduce reaction rate to some extent, the activation effect of nFe^0 is still better than Fe^0 and Fe^{2+} (Al-Shamsi & Thomson 2013).

$$Fe^0_{(s)} + SO_4^{2-} + 2H_2O \rightarrow FeSO_{4(s)} + 2OH^- + H_{2(g)} \quad (42)$$

$$FeOOH_{(s)} + SO_4^{2-} + H_2O \rightarrow FeSO_{4(s)} + 2OH^- + 1/2H_{2(g)} + 1/2O_2(g) \quad (43)$$

Compared with the funding of Al-Shamsi & Thomson (2013), Kim *et al.* (2018) used XRD and SEM-EDS to analyze surface composition of nFe^0 when the reaction was initiating in the Fe^0/PS system, and it was found that both lepidocrocite (FeOOH) and schwertmannite ($Fe_8O_8(OH)_6SO_{4(s)}$) were formed on the nFe^0 surface, and the reaction were as Equations (44) and (45).

$$Fe^{3+} + 2H_2O \leftrightarrow FeOOH_{(s)} + 3H^+ \quad (44)$$

$$8Fe^{3+} + SO_4^{2-} + 14H_2O \leftrightarrow Fe_8O_8(OH)_6SO_{4(s)} + 22H^+ \quad (45)$$

As reaction time increase, FeOOH reacted with nFe^0 to form magnetite (Fe_3O_4) through electron transfer of bulk conduction. Simultaneously, the internal Fe^0 volume continued to shrink, and released Fe^{2+} and Fe^{3+}. Kim *et al.* (2018) proposed a model of core-shell structure (Figure 1) including Fe^0(s) core, the inner layer Fe_3O_4, and the outer layer Fe^{3+}. Moreover, they found that nFe^0 can release Fe^{2+} for PS at a very fast rate, which is faster than Fe^0 under optimal conditions.

Nanosized zero-valent iron/support materials

Although nFe^0 has a better effectiveness in activating PS for refractory organics degradation owing to its small particle size, large surface area and high reactivity, its application still faced some practical problems (Fu *et al.* 2014). Mueller *et al.* (2012), Fu *et al.* (2014) and Stefaniuk *et al.* (2016) all found that high surface energies and inherent magnetism of nFe^0 lead to agglomerating of nFe^0 particles, which limits the mobility of nFe^0 and reduces electron transfer of nFe^0. In addition, nFe^0 is easily oxidized by the oxygen as it is exposed to the air, lack of stability and difficulty separating from the water is problematic in terms of practical application. In order to solve the weaknesses of nFe^0 particles, some materials (such as biochar (BC), reduced graphene oxide (rGO), mesoporous carbon (MC) and montmorillonite) have been used to support nFe^0.

Biochar (BC) is a low-cost carbonaceous adsorbent generated in an oxygen-limited or oxygen-free environment at high temperatures by pyrolysis of biomass (Yan *et al.* 2015; Xu *et al.* 2018b; Luo *et al.* 2019; Park *et al.* 2019; Wang *et al.* 2019a, 2019d). BC has a strong adsorption capacity due to its high surface area (SA)-to-volume ratio and porous properties (Wei *et al.* 2018; Wang *et al.* 2019b).

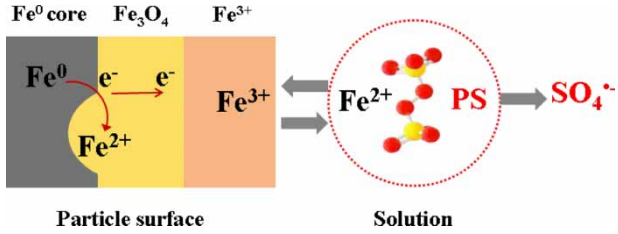

Figure 1 | Schematic illustration of multi-layered core-shell structure of nFe^0.

Ahmed *et al.* (2016) and Ravikumar *et al.* (2018) found the surface of BC contains abundant oxygen-rich functional groups (such as hydroxyl (–OH) and carboxyl (–COOH)) which can quickly adsorb organic contaminants. Han *et al.* (2015b) testified because of these unique properties of these functional groups, BC has been used as mechanical supporting material for nFe^0 to disperse and stabilize nFe^0. In detail, BC has a large specific surface area and a large number of micropores, which can provide a support carbon skeleton for nFe^0 to immobilize (Liu *et al.* 2018; Wang *et al.* 2019d). nFe^0 is stabilized on surface of BC via adsorption, coordination, chelation and bridging (Jiang *et al.* 2019; Wang *et al.* 2019d).

Some researchers inferred the PS activation mechanisms in nFe^0/BC/PS system, and the basic mechanisms are illustrated as follows (Yan *et al.* 2015; Xu *et al.* 2018b; Luo *et al.* 2019; Park *et al.* 2019). (1) As nFe^0 disperses well on BC surface, Fe^{2+}, gradually formed by oxidation of nFe^0, activates PS to form $SO_4^{\bullet-}$. (2) Nano-Fe^0 directly activates PS to generate $SO_4^{\bullet-}$ and $HO^{\bullet}$ based on Equations (46) and (47). (3) The appearance of ferrous sulfate may induce PS decomposition. Al-Shamsi & Thomson (2013) proposed that ferrous sulfate might be formed on the nFe^0 surface in two ways. One way is that Fe^0 and SO_4^{2-} in solution form $FeSO_4$ (Equation (48)). In the other way, under anaerobic conditions, Fe^{3+} is formed via oxidation of Fe^{2+} (Equation (49)). $Fe(OH)_3$ is formed as an intermediate (Equations (50) and (51)), then generates FeOOH (Equation (52)) which can react with SO_4^{2-} in solution to generate $FeSO_4$ (Equation (53)). (4) Except for BC surface adsorption, BC abundant oxygen functional groups of C-OOH and C-OH on the surface can directly catalyze PS to generate $SO_4^{\bullet-}$ for degradation of refractory organics (Equations (54) and (55)) (Yan *et al.* 2015; Zhou *et al.* 2015; Tan *et al.* 2016; Xu *et al.* 2018b; Zhang *et al.* 2018a).

$$Fe^0 + 2S_2O_8^{2-} \rightarrow Fe^{2+} + 2SO_4^{\bullet-} + 2SO_4^{2-} \quad (46)$$

$$Fe^0 + S_2O_8^{2-} + 2H_2O \rightarrow Fe^{2+} + 2SO_4^{2-} + 2^{\bullet}OH + 2H^+ \quad (47)$$

$$Fe^0 + SO_4^{2-} + 2H_2O \rightarrow FeSO_{4(S)} + 2OH^- + H_2 \quad (48)$$

$$Fe^{2+} + H_2O \rightarrow Fe^{3+} + OH^- + 1/2H_2 \quad (49)$$

$$Fe^{3+} + 3OH^- \rightarrow Fe(OH)_3 \quad (50)$$

$$Fe^{3+} + 3H_2O \rightarrow Fe(OH)_3 + 3H^+ \quad (51)$$

$$Fe(OH)_3 \rightarrow FeOOH + H_2O \quad (52)$$

$$FeOOH + SO_4^{2-} + H_2O \rightarrow FeSO_{4(s)} + 2OH^- + H_2 + O_2 \quad (53)$$

$$BC - OOH + S_2O_8^{2-} \rightarrow BC - OO^{\bullet} + SO_4^{\bullet-} + HSO_4^- \quad (54)$$

$$BC - OH + S_2O_8^{2-} \rightarrow BC - O^{\bullet} + SO_4^{\bullet-} + HSO_4^- \quad (55)$$

Reduced graphene oxide (rGO), is a two-dimensional monolayer with abundant sp^2-bonded carbon. It is a versatile matrix used as a support for nFe^0 nanoparticles (Yang *et al.* 2015; Hao *et al.* 2018; Soubh *et al.* 2018; Xu *et al.* 2018a). Owing to the layered structure, rGO has a large specific surface area that provides abundant adsorption sites for the immobilization of nFe^0. The mechanism of activating PS in nFe^0/rGO is similar to that of nFe^0/BC. Except for providing support for nFe^0, the functional groups such as –OOH and –OH on rGO surface can also catalyze PS to release organic radicals and sulfate radicals, seen as Equations (56) and (57) (Duan *et al.* 2015; Wu *et al.* 2018).

$$GR - OOH + S_2O_8^{2-} \rightarrow GR - OO^{\bullet} + SO_4^{\bullet-} + HSO_4^- \quad (56)$$

$$GR - OH + S_2O_8^{2-} \rightarrow GR - O^{\bullet} + SO_4^{\bullet-} + HSO_4^- \quad (57)$$

Ahmad *et al.* (2015) had investigated different types of reactive oxygen species (ROS) generated in the nFe^0/rGO/PS system. Because of their different reaction rate constant, tert-Butanol, NB, AN, and CT were employed as probe compounds to identify $HO^{\bullet}$, $HO^{\bullet}$, both $HO^{\bullet}$ and $SO4^{\bullet-}$, and $O_2^{\bullet-}$, respectively. The result proves the presence of three free radicals in the nFe^0/rGO/PS system. In acidic conditions, more $SO_4^{\bullet-}$ radicals were generated compared to $HO^{\bullet}$ radicals, while $O_2^{\bullet-}$ radicals prefer a basic condition. In order to avoid the leakage of nFe^0 and promote the tight adhesion of nFe^0 on RGO, polydopamine (PDA), as a polymeric stabilizer, has been studied to use as nFe^0 coating. PDA has a specialized adhesive foot protein and can adhere on nFe^0 surface to modify nFe^0 due to abundant functional groups possessing strong negative charge with the ability to bind positively charged iron. A study by Gu *et al.* (2018) has also confirmed that the nFe^0/PDA/rGO/PS system showed better performance on pollutants removal than the nFe^0/rGO/PS system owing to the presence of PDA. Jiang *et al.* (2018) investigated removal efficiency of TC in different systems, the removal rate of TC in descending order

is: nFe^0/MC/PS > MC/PS > MC > nFe^0/MC > nFe^0/PS > nFe0 > PS. The highest removal efficiency (92.1%) was obtained in the nFe^0/MC/PS system. This could attribute to a synergistic effect between Fe^0 and MC. Besides, the reaction mechanism of the nFe^0/MC/PS system is similar to that of the Fe^0/MC/PS system.

In addition, montmorillonite (Mt) as naturally abundant mineral clay has been investigated for support nFe^0 to activate PS in degrading refractory organics (Wu *et al.* 2019) because of its high specific surface area and cation exchange capacity. Cationic surfactant-modified Mt (organo-montmorillonite, OMt) is more hydrophobic and has showed better catalytic performance than Mt (Wu *et al.* 2019).

SOME IRON-CONTAINING COMPOUNDS

Some iron-containing compounds such as hematite (Fe_2O_3), magnetite (Fe_3O_4), and ferrous sulfide (FeS), are also explored to activate PS for refractory organics degradation.

Teel *et al.* (2011) evaluated the effects of several soil minerals including hematite on PS activation and found that hematite is capable of activating PS for removal organic pollutants in water. This effect is attributed to the octahedral sites of hematite containing Fe^{2+} that can react with PS to produce $SO_4^{\bullet-}$, according to Equation (1). Figure 2 illustrates the activated mechanism in which PS is activated to generate sulfate radicals for degradation of organic pollutants. The mechanism of the activation of PS by hematite is similar to that by Fe^{2+}, but due to the heterogeneous catalysis of hematite, catalytic reactions will occur both on the surface of the Fe_2O_3 and in the solution. Firstly, Fe^{2+} at some sites on the surface of the hematite will adsorb PS in aqueous solution, then react with PS to form $SO_4^{\bullet-}$, SO_4^{2-} and Fe^{3+}. Fe^{3+} also reacts with PS to form Fe^{2+}, which forms a cycle between Fe^{2+} and Fe^{3+} on the surface of hematite. The Fe^{2+} and Fe^{3+} leaking into the solution also undergo the same cyclic reaction as the surface. There is also the formation of $SO_4^{\bullet-}$ during this cycle. $SO_4^{\bullet-}$ formed on the surface of hematite or in the solution can capture and react contaminants to form by-products in water, which ultimately produce carbon dioxide and water. Free radical scavenging experiment in reference (Kermani *et al.* 2018) have shown that there is also $HO^{\bullet}$ that could be generated during oxidation of PS by hematite; $HO^{\bullet}$ also plays a role on degradation of refractory organics. The type of free radicals generated in PS/Fe_2O_3 system are determined by solution pH and the type of targeting contaminants. $SO_4^{\bullet-}$ are usually dominant under an acidic condition, while $HO^{\bullet}$ prefers a neutral and alkaline environment.

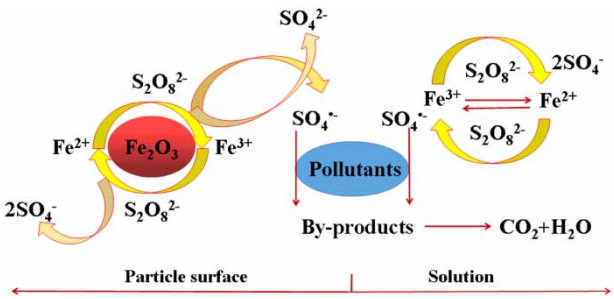

Figure 2 | Diagram of the mechanism of Fe_2O_3 catalyzing persulfate.

Magnetite nanoparticles (MNPs) have also been studied as a catalyst similar to hematite because they can work under mild reaction conditions and be easily separated and recovered. Magnetite is a magnetic particle, and nanometer magnetite can be synthesized by reverse co-precipitation among $FeCl_3{\cdot}6H_2O + FeSO_4{\cdot}4H_2O + NH_3{\cdot}H_2O$. Literature (Leng *et al.* 2013, 2014; Sun *et al.* 2016; Zhu *et al.* 2018) demonstrated that treatment effects, reaction conditions and mechanisms of different types of synthetic Fe_3O_4 and its complexes with other materials (biochar, NrGO) to activate PS for effectively degradation of refractory organics. Magnetite contains Fe^{2+}, which can stimulate decomposition of PS to generate free radicals. However, the Fe^{2+} may have not enough magnetite due to the slow transformation between Fe^{2+} and Fe^{3+} cycles. As a result, modifying surfaces of Fe_3O_4 MNPs and improving the redox cycle of Fe^{2+}/Fe^{3+} is a very important research issue (Sun *et al.* 2016). Some studies investigated polyhydroquinone-coated Fe_3O_4, ascorbic acid modified Fe_3O_4, β-CD immobilized Fe_3O_4 as catalysts for the activation of PS (Leng *et al.* 2013, 2014; Sun *et al.* 2016; Zhu *et al.* 2018). According to Sun *et al.* (2016), ascorbic acid (H_2A, also called vitamin C), a redox mediator, used to modify Fe_3O_4 MNPs could enhance the ability of activating PS. Under same conditions, the effect of H_2A/Fe_3O_4 on PS activation was greater than that of Fe_3O_4 alone on PS activation. Under H_2A/Fe_3O_4 activation, a removal rate (98.5%) of 2,4-DCP can be obtained, while only 35.1% degradation of 2,4-DCP was achieved in Fe_3O_4/PS system, which was testified that the introduction of H_2A in Fe_3O_4/PS can effectively activate PS for targeting pollutants removal. Nowack (2002) and Dong *et al.* (2017) all testified that H_2A is an effective chelating and reducing agent that can enhance iron ions released from minerals. The primary mechanism of improved refractory organics degradation in the H_2A/Fe_3O_4/PS process is illustrated in Figure 3. First, H_2A, as a chelating agent, attached on surface of Fe_3O_4

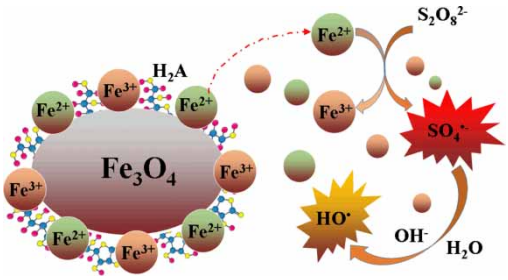

Figure 3 | Primary mechanism occurred in the H_2A/ Fe_3O_4/PS process.

particles combines with Fe^{2+} to form chelated iron of Fe^{2+}–H_2A through the ligand exchange reaction. Then, Fe^{2+} enters into aqueous phase initiating a reaction that catalyzes PS to generate $SO_4^{\cdot-}$. In addition, H_2A can enhance the performance of reduction of Fe^{3+} to Fe^{2+} on the Fe_3O_4 nanoparticle surface and promote more release of Fe^{2+} from Fe_3O_4 into solution.

Compared with homogenous Fe^{2+}/PS system, heterogeneous FeS/PS system also shows a good performance on refractory organics removal (Pu *et al.* 2014; Yuan *et al.* 2015; Zhang *et al.* 2017; Fan *et al.* 2018). Yuan *et al.* (2015) found that the application ranges of pH for p-chloroaniline (PCA) fast degradation was from 3.0 to 7.0, while the optimum pH range was from 5.0 to 7.0 for complete degradation of PCA at 150 min according the research of Fan *et al.* (2018). The PS activation mechanism was affected by the initial solution pH. The mechanism of FeS activating PS is shown in Figure 4. As a solid particle like Fe^0, FeS could continuously release dissolved Fe^{2+} (Yuan *et al.* 2015) which would activate PS to produce $SO_4^{\cdot-}$. In addition, as an electron donor, S^{2+} was able to reduce Fe^{3+} to Fe^{2+} (Fan *et al.* 2018). Sustainable release of Fe^{2+} and recycling of Fe^{3+} by FeS during reaction could avoid surplus Fe^{2+} consumption and Fe^{3+} accumulation. Based on this mechanism, when the initial solution pH was 9.0–11.0, the dissolved Fe^{2+} from FeS was not enough to activate PS and relatively low PCA removal rate was acquired.

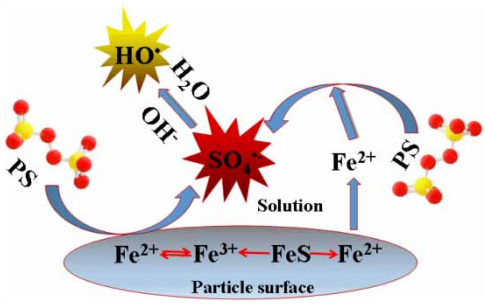

Figure 4 | Schematic diagram of the mechanism of FeS activating PS.

ECONOMIC EVALUATION

Regarding the methods for iron-based materials to activate PS to degrade organics, we are not only concerned with the efficiency, but also with the cost. Since these methods have not yet been applied in engineering, the cost of chemical agents in small experiments based on different iron materials is calculated and analyzed according to the consumption and price of chemical agents. Table 4 shows the unit price of iron-based materials found on the website of Sigma. Table 5 lists the experimental data such as oxide and catalyst concentration and removal efficiency in several representative small experiments, and also shows the cost of processing 1 L of water after calculation (in US dollars). The cost of each process is the sum of the cost of the catalyst and the oxidizing agent used to achieve an organic removal rate of more than 95%. According to the calculation results, the order of chemical costs from high to low is Fe_3O_4/PS, nFe^0/PS, $FeSO_4{\cdot}7H_2O$/PS, FeS/PS, Fe_2O_3/PS, and Fe^0/PS. Since the price of the analytical reagent is used as a unit price, the calculation cost is high, and the cost will be reduced in actual engineering. In addition, the difference in the degree of difficult degradation of pollutants also determines that the same system will generate different treatment costs. These data are for reference only for small experimental chemistry costs.

CONCLUSION AND PROSPECTS

In summary, a state-of-the-art review is presented on mechanisms, reaction conditions, influencing factors, and treatment effects of iron-based materials for refractory organics degradation via PS activation. The results of recently published articles affirm that activated-PS by

Table 4 | Unit price of iron-based materials

Molecular formula	Unit price USD/kg	Molecular weight	Size	CAS number
$FeSO_4{\cdot}7H_2O$	166	278.01		7782-63-0
$Na_2S_2O_8$	43.2	238.1		7775-27-1
$K_2S_2O_8$	170.4	270.32		7727-21-1
Fe^0	92	55.85	325 mesh	7439-89-6
Nano-Fe^0	7,760	55.85	60–80 nm	7439-89-6
Fe_2O_3	66	159.69	<5 μm	1309-37-1
Fe_3O_4	566	231.53	<5 μm	1317-61-9
FeS	264.4	87.91		1317-37-9

Table 5 | The parameters and costs of the iron-based processes

Catalytic system	Parameters	Costs (USD/L)	Reference
Fe^{2+}/PS	$[Na_2S_2O_8]$ = 4.385 mM, $[Fe^{2+}]$ = 2.1925 mM, [BPA] = 0.0876 mM, pH = 7.0, 100%	0.146	Gao *et al.* (2018)
Fe^0/PS	$[Na_2S_2O_8]$ = 4.385 mM, $[Fe^0]$ = 2.1925 mM, [BPA] = 0.0876 mM, pH = 7.0, 100%	0.056	Gao *et al.* (2018)
nFe^0/PS	$[Na_2S_2O_8]$ = 1 mM,$[nFe^0]$ = 28 mg/L, [SMT] = 10 mg/L, pH = 5.3, 100%	0.227	Lin & Chen (2018)
Fe_2O_3/PS	$[Na_2S_2O_8]$ = 10 mM,$[Fe_2O_3]$ = 0.1 g/L, [OG] = 0.1 mM, pH = 5.0, 95.0%	0.110	Ike *et al.* (2018)
Fe_3O_4/PS	$[K_2S_2O_8]$ = 1.2 mM,$[Fe_3O_4]$ = 2.4 mM, [SMM] = 0.06 mM, pH = 6.4, 96.0%	0.369	Yan *et al.* (2011)
FeS/PS	$[Na_2S_2O_8]$ = 4 mM,[FeS] = 0.35 g/L, [PCA] = 0.2 mM, pH = 3.0, 97.3%	0.133	Fan *et al.* (2018)

iron-based materials has promising potentials for destruction of refractory organics in water and 100% degradation can be accomplished for some refractory organics under optimized conditions. However, challenges still remain in the improvement of refractory organics degradation rate in actual polluted water treatment using iron-based materials/PS processes, and the practical engineering application of these processes with low costs is also highly anticipated.

The activation performance of iron-based materials can be influenced by the properties and concentrations of activators, pollutants, oxidants, and water quality component along with the reaction conditions (such as pH, temperature, reaction time). Optimization of the experimental conditions is a cornerstone in achieving best removal. Deep research on environmentally friendly iron-chelators will help to increase Fe^0 functional lifespan and improve removal rate of refractory organics in Fe^0/PS system. Without a doubt, nFe^0 shows the most promise for PS activation if the problems of nFe^0 leakage and accumulation can be properly solved. BC and rGO as effective supports for nFe^0 can reduce nFe^0 leakage, but the increased cost should be taken into account in future engineering applications. Moreover, it is also necessary to optimize the nFe^0/BC/PS or nFe^0/rGO/PS process from the perspective of reaction kinetics and other reaction conditions. Other iron-containing materials (Fe_2O_3, Fe_3O_4, FeS, etc.) also are used in the catalysis activation mechanism of Fe^{2+} to activate PS. Therefore, the key issue is to identify the factors that affect the release of Fe^{2+} and maintain a dynamic balance between Fe^{2+} and Fe^{3+} when using these materials as activators. Novel reactor for the iron-based materials/PS system based on batch or continuous flow need to designed, and more pilot experiments have yet to be implemented.

In a word, because of the low cost, availability, and environmental friendliness of iron, iron-based materials activation method for PS is expected to have a better prospect with further research in this field.

ACKNOWLEDGEMENT

The research group acknowledges the financial support provided by the Natural Sciences and Engineering Research Council (NSERC) of Canada through the CREATE, Discovery and CRD programs and Queen's University. Pascale Champagne is thankful to the Canada Research Chairs Program. Yanjiao Gao thanks the China Scholarship Council for funding a visiting scholar (201808210024). Tiehong Song expresses gratitude for the funding (JJKH20200288KJ) of Jilin Province Education Department of China.

REFERENCES

Ahmad, A., Gu, X., Li, L., Lu, S., Xu, Y. & Guo, X. 2015 Effects of pH and anions on the generation of reactive oxygen species (ROS) in nZVI-rGO-activated persulfate system. *Water, Air, & Soil Pollution* **226** (11), 369. https://doi.org/10.1007/s11270-015-2635-8.

Ahmadpour, E. & Yengejeh, R. J. 2016 Application of a zero-valente iron-per sulfate system to treat petrochemical wastewater with high-total dissolved solids containing para-chlorophenol. *Jundishapur Journal of Health Sciences* **8** (2). https://doi.org/10.17795/jjhs-35108.

Ahmed, M. B., Zhou, J. L., Ngo, H. H., Guo, W. & Chen, M. 2016 Progress in the preparation and application of modified biochar for improved contaminant removal from water and wastewater. *Bioresource Technology* **214**, 836–851. https://doi.org/10.1016/j.biortech.2016.05.057.

Al-Shamsi, M. A. & Thomson, N. R. 2013 Treatment of organic compounds by activated persulfate using nanoscale zerovalent iron. *Industrial & Engineering Chemistry Research* **52** (38), 13564–13571. https://doi.org/10.1021/ie400387p.

Amasha, M., Baalbaki, A. & Ghauch, A. 2018 A comparative study of the common persulfate activation techniques for the complete degradation of an NSAID: the case of ketoprofen. *Chemical Engineering Journal* **350**, 395–410. https://doi.org/10.1016/j.cej.2018.05.118.

Babuponnusami, A. & Muthukumar, K. 2011 Degradation of phenol in aqueous solution by Fenton, sono-Fenton and sono-photo-Fenton methods. *Clean–Soil, Air, Water* **39** (2), 142–147. https://doi.org/10.1002/clen.201000072.

Brienza, M. & Katsoyiannis, I. 2017 Sulfate radical technologies as tertiary treatment for the removal of emerging contaminants from wastewater. *Sustainability* **9** (9), 1604. https://doi.org/10.3390/su9091604.

Bu, L., Shi, Z. & Zhou, S. 2016 Modeling of Fe(II)-activated persulfate oxidation using atrazine as a target contaminant. *Separation and Purification Technology* **169**, 59–65. https://doi.org/10.1016/j.seppur.2016.05.037.

Bu, L., Bi, C., Shi, Z. & Zhou, S. 2017 Significant enhancement on ferrous/persulfate oxidation with epigallocatechin-3-gallate: simultaneous chelating and reducing. *Chemical Engineering Journal* **321**, 642–650. https://doi.org/10.1016/j.cej.2017.04.001.

Cao, J., Zhang, W. X., Brown, D. G. & Sethi, D. 2008 Oxidation of lindane with Fe(II)-activated sodium persulfate. *Environmental Engineering Science* **25** (2), 221–228. https://doi.org/10.1089/ees.2006.0244.

Caré, S., Crane, R., Calabrò, P. S., Ghauch, A., Temgoua, E. & Noubactep, C. 2013 Modeling the permeability loss of metallic iron water filtration systems. *Clean–Soil, Air, Water* **41** (3), 275–282. https://doi.org/10.1002/clen.201200167.

Chen, J., Feng, J., Lu, S., Shen, Z., Du, Y., Peng, L., Nian, P., Yuan, S. & Zhang, A. 2018 Non-thermal plasma and Fe^{2+} activated persulfate ignited degradation of aqueous crystal violet: degradation mechanism and artificial neural network modeling. *Separation and Purification Technology* **191**, 75–85. https://doi.org/10.1016/j.seppur.2017.09.016.

Cheng, X., Guo, H., Zhang, Y., Wu, X. & Liu, Y. 2017 Non-photochemical production of singlet oxygen via activation of persulfate by carbon nanotubes. *Water Research* **113**, 80–88. https://doi.org/10.1016/j.watres.2017.02.016.

Csay, T., Homlok, R., Illes, E., Takacs, E. & Wojnarovits, L. 2014 The chemical background of advanced oxidation processes. *Israel Journal of Chemistry* **54** (3), 233–241. https://doi.org/10.1002/ijch.201300077.

Darsinou, B., Frontistis, Z., Antonopoulou, M., Konstantinou, I. & Mantzavinos, D. 2015 Sono-activated persulfate oxidation of bisphenol A: kinetics, pathways and the controversial role of temperature. *Chemical Engineering Journal* **280**, 623–633. https://doi.org/10.1016/j.cej.2015.06.061.

Deng, Y. & Zhao, R. 2015 Advanced oxidation processes (AOPs) in wastewater treatment. *Current Pollution Reports* **1** (3), 167–176. https://doi.org/10.1007/s40726-015-0015-z.

Deng, J., Shao, Y., Gao, N., Deng, Y., Tan, C. & Zhou, S. 2014 Zero-valent iron/persulfate (Fe^0/PS) oxidation acetaminophen in water. *International Journal of Environmental Science and Technology* **11** (4), 881–890. https://doi.org/10.1007/s13762-013-0284-2.

Ding, F., Chen, H., Zhang, S., Zhao, T. & Liu, N. 2017 Effect of chelating agents on Reactive Green 19 decolorization through Fe^0-activated persulfate oxidation process. *Journal of Environmental Management* **200**, 325–334. https://doi.org/10.1016/j.jenvman.2017.05.089.

Dong, H., Qiang, Z., Hu, J. & Sans, C. 2017 Accelerated degradation of iopamidol in iron activated persulfate systems: roles of complexing agents. *Chemical Engineering Journal* **316**, 288–295. https://doi.org/10.1016/j.cej.2017.01.099.

Duan, X., Sun, H., Kang, J., Wang, Y., Indrawirawan, S. & Wang, S. 2015 Insights into heterogeneous catalysis of persulfate activation on dimensional-structured nanocarbons. *Acs Catalysis* **5** (8), 4629–4636. https://doi.org/10.1021/acscatal.5b00774.

Epold, I., Trapido, M. & Dulova, N. 2015 Degradation of levofloxacin in aqueous solutions by Fenton, ferrous ion-activated persulfate and combined Fenton/persulfate systems. *Chemical Engineering Journal* **279**, 452–462. https://doi.org/10.1016/j.cej.2015.05.054.

Fan, J., Gu, L., Wu, D. & Liu, Z. 2018 Mackinawite (FeS) activation of persulfate for the degradation of p-chloroaniline: surface reaction mechanism and sulfur-mediated cycling of iron species. *Chemical Engineering Journal* **333**, 657–664. https://doi.org/10.1016/j.cej.2017.09.175.

Fast, S. A., Gude, V. G., Truax, D. D., Martin, J. & Magbanua, B. S. 2017 A critical evaluation of advanced oxidation processes for emerging contaminants removal. *Environmental Processes* **4** (1), 283–302. https://doi.org/10.1007/s40710-017-0207-1.

Fu, F., Dionysiou, D. D. & Liu, H. 2014 The use of zero-valent iron for groundwater remediation and wastewater treatment: a review. *Journal of Hazardous Materials* **267**, 194–205. https://doi.org/10.1016/j.jhazmat.2013.12.062.

Gao, F., Li, Y. & Xiang, B. 2018 Degradation of bisphenol A through transition metals activating persulfate process. *Ecotoxicology and Environmental Safety* **158**, 239–247. https://doi.org/10.1016/j.ecoenv.2018.03.035.

Ghatak, H. R. 2014 Advanced oxidation processes for the treatment of biorecalcitrant organics in wastewater. *Critical Reviews in Environmental Science and Technology* **44** (11), 1167–1219. https://doi.org/10.1080/10643389.2013.763581.

Ghauch, A. 2008 Rapid removal of flutriafol in water by zero-valent iron powder. *Chemosphere* **71** (5), 816–826. https://doi.org/10.1016/j.chemosphere.2007.11.057.

Ghauch, A. 2015 Iron-based metallic systems: an excellent choice for sustainable water treatment. *FOG-Freiberg Online Geoscience* **38**, 1–80.

Ghauch, A. & Tuqan, A. 2008 Catalytic degradation of chlorothalonil in water using bimetallic iron-based systems. *Chemosphere* **73** (5), 751–759. https://doi.org/10.1016/j.chemosphere.2008.06.035.

Ghauch, A. & Tuqan, A. 2009 Reductive destruction and decontamination of aqueous solutions of chlorinated antimicrobial agent using bimetallic systems. *Journal of Hazardous Materials* **164** (2–3), 665–674. https://doi.org/10.1016/j.jhazmat.2008.08.048.

Ghauch, A. & Tuqan, A. M. 2012 Oxidation of bisoprolol in heated persulfate/H_2O systems: kinetics and products. *Chemical Engineering Journal* **183**, 162–171. https://doi.org/10.1016/j.cej.2011.12.048.

Ghauch, A., Tuqan, A. & Assi, H. A. 2009 Antibiotic removal from water: elimination of amoxicillin and ampicillin by microscale and nanoscale iron particles. *Environmental*

Pollution **157** (5), 1626–1635. https://doi.org/10.1016/j.envpol.2008.12.024.

Ghauch, A., Assi, H. A. & Bdeir, S. 2010a Aqueous removal of diclofenac by plated elemental iron: bimetallic systems. *Journal of Hazardous Materials* **182** (1–3), 64–74. https://doi.org/10.1016/j.jhazmat.2010.05.139.

Ghauch, A., Assi, H. A. & Tuqan, A. 2010b Investigating the mechanism of clofibric acid removal in Fe^0/H_2O systems. *Journal of Hazardous Materials* **176** (1–3), 48–55. https://doi.org/10.1016/j.jhazmat.2009.10.125.

Ghauch, A., Assi, H. A., Baydoun, H., Tuqan, A. M. & Bejjani, A. 2011a Fe^0-based trimetallic systems for the removal of aqueous diclofenac: mechanism and kinetics. *Chemical Engineering Journal* **172** (2–3), 1033–1044. https://doi.org/10.1016/j.cej.2011.07.020.

Ghauch, A., Baydoun, H. & Dermesropian, P. 2011b Degradation of aqueous carbamazepine in ultrasonic/Fe^0/H_2O_2 systems. *Chemical Engineering Journal* **172** (1), 18–27. https://doi.org/10.1016/j.cej.2011.04.002.

Ghauch, A., Ayoub, G. & Naim, S. 2013 Degradation of sulfamethoxazole by persulfate assisted micrometric Fe^0 in aqueous solution. *Chemical Engineering Journal* **228**, 1168–1181. https://doi.org/10.1016/j.cej.2013.05.045.

Graça, C. A., de Velosa, A. C. & Teixeira, A. C. S. 2017 Amicarbazone degradation by UVA-activated persulfate in the presence of hydrogen peroxide or Fe^{2+}. *Catalysis Today* **280**, 80–85. https://doi.org/10.1016/j.cattod.2016.06.044.

Gu, X., Lu, S., Guo, X., Sima, J., Qiu, Z. & Sui, Q. 2015 Oxidation and reduction performance of 1,1,1-trichloroethane in aqueous solution by means of a combination of persulfate and zero-valent iron. *RSC Advances* **5** (75), 60849–60856. https://doi.org/10.1039/C5RA07655B.

Gu, M., Sui, Q., Farooq, U., Zhang, X., Qiu, Z. & Lyu, S. 2018 Degradation of phenanthrene in sulfate radical based oxidative environment by nZVI-PDA functionalized rGO catalyst. *Chemical Engineering Journal* **354**, 541–552. https://doi.org/10.1016/j.cej.2018.08.039.

Guerra-Rodríguez, S., Rodríguez, E., Singh, D. N. & Rodríguez-Chueca, J. 2018 Assessment of sulfate radical-based advanced oxidation processes for water and wastewater treatment: a review. *Water* **10** (12), 1828. https://doi.org/10.3390/w10121828.

Guo, Y., Zhou, J., Lou, X., Liu, R., Xiao, D., Fang, C., Wang, Z. & Liu, J. 2014 Enhanced degradation of Tetrabromobisphenol A in water by a UV/base/persulfate system: kinetics and intermediates. *Chemical Engineering Journal* **254**, 538–544. https://doi.org/10.1016/j.cej.2014.05.143.

Han, D., Wan, J., Ma, Y., Wang, Y., Huang, M., Chen, Y., Li, D., Guan, Z. & Li, Y. 2014 Enhanced decolorization of Orange G in a Fe(II)-EDDS activated persulfate process by accelerating the regeneration of ferrous iron with hydroxylamine. *Chemical Engineering Journal* **256**, 316–323. https://doi.org/10.1016/j.cej.2014.06.006.

Han, D., Wan, J., Ma, Y., Wang, Y., Li, Y., Li, D. & Guan, Z. 2015a New insights into the role of organic chelating agents in Fe(II) activated persulfate processes. *Chemical Engineering Journal* **269**, 425–433. https://doi.org/10.1016/j.cej.2015.01.106.

Han, L., Xue, S., Zhao, S., Yan, J., Qian, L. & Chen, M. 2015b Biochar supported nanoscale iron particles for the efficient removal of methyl orange dye in aqueous solutions. *PLoS One* **10** (7). https://doi.org/10.1371/journal.pone.0132067.

Hao, J., Ji, L., Li, C., Hu, C. & Wu, K. 2018 Rapid, efficient and economic removal of organic dyes and heavy metals from wastewater by zinc-induced in-situ reduction and precipitation of graphene oxide. *Journal of the Taiwan Institute of Chemical Engineers* **88**, 137–145. https://doi.org/10.1016/j.jtice.2018.03.045.

Hussain, I., Zhang, Y., Huang, S. & Du, X. 2012 Degradation of p-chloroaniline by persulfate activated with zero-valent iron. *Chemical Engineering Journal* **203**, 269–276. https://doi.org/10.1016/j.cej.2012.06.120.

Hussain, I., Zhang, Y. & Huang, S. 2014 Degradation of aniline with zero-valent iron as an activator of persulfate in aqueous solution. *RSC Advances* **4** (7), 3502–3511. https://doi.org/10.1039/C3RA43364A.

Ike, I. A., Linden, K. G., Orbell, J. D. & Duke, M. 2018 Critical review of the science and sustainability of persulphate advanced oxidation processes. *Chemical Engineering Journal* **338**, 651–669. https://doi.org/10.1016/j.cej.2018.01.034.

Ioan, I., Wilson, S., Lundanes, E. & Neculai, A. 2007 Comparison of Fenton and sono-Fenton bisphenol A degradation. *Journal of Hazardous Materials* **142** (1–2), 559–563. https://doi.org/10.1016/j.jhazmat.2006.08.015.

Ji, Y., Ferronato, C., Salvador, A., Yang, X. & Chovelon, J. M. 2014 Degradation of ciprofloxacin and sulfamethoxazole by ferrous-activated persulfate: implications for remediation of groundwater contaminated by antibiotics. *Science of the Total Environment* **472**, 800–808. https://doi.org/10.1016/j.scitotenv.2013.11.008.

Ji, Y., Dong, C., Kong, D., Lu, J. & Zhou, Q. 2015 Heat-activated persulfate oxidation of atrazine: implications for remediation of groundwater contaminated by herbicides. *Chemical Engineering Journal* **263**, 45–54. https://doi.org/10.1016/j.cej.2014.10.097.

Ji, Q., Li, J., Xiong, Z. & Lai, B. 2017 Enhanced reactivity of microscale Fe/Cu bimetallic particles (mFe/Cu) with persulfate (PS) for p-nitrophenol (PNP) removal in aqueous solution. *Chemosphere* **172**, 10–20. https://doi.org/10.1016/j.chemosphere.2016.12.128.

Jiang, X., Wu, Y., Wang, P., Li, H. & Dong, W. 2013 Degradation of bisphenol A in aqueous solution by persulfate activated with ferrous ion. *Environmental Science and Pollution Research* **20** (7), 4947–4953. https://doi.org/10.1007/s11356-013-1468-5.

Jiang, X., Guo, Y., Zhang, L., Jiang, W. & Xie, R. 2018 Catalytic degradation of tetracycline hydrochloride by persulfate activated with nano Fe0 immobilized mesoporous carbon. *Chemical Engineering Journal* **341**, 392–401. https://doi.org/10.1016/j.cej.2018.02.034.

Jiang, S. F., Ling, L. L., Chen, W. J., Liu, W. J., Li, D. C. & Jiang, H. 2019 High efficient removal of bisphenol A in a peroxymonosulfate/iron functionalized biochar system: mechanistic elucidation and quantification of the contributors. *Chemical Engineering Journal* **359**, 572–583. https://doi.org/10.1016/j.cej.2018.11.124.

Kambhu, A., Gren, M., Tang, W., Comfort, S. & Harris, C. E. 2017 Remediating 1, 4-dioxane-contaminated water with slow-release persulfate and zerovalent iron. *Chemosphere* **175**, 170–177. https://doi.org/10.1016/j.chemosphere.2017.02.044.

Kang, J., Duan, X., Wang, C., Sun, H., Tan, X., Tade, M. O. & Wang, S. 2018 Nitrogen-doped bamboo-like carbon nanotubes with Ni encapsulation for persulfate activation to remove emerging contaminants with excellent catalytic stability. *Chemical Engineering Journal* **332**, 398–408. https://doi.org/10.1016/j.cej.2017.09.102.

Kermani, M., Mohammadi, F., Kakavandi, B., Esrafili, A. & Rostamifasih, Z. 2018 Simultaneous catalytic degradation of 2, 4-D and MCPA herbicides using sulfate radical-based heterogeneous oxidation over persulfate activated by natural hematite (α-Fe_2O_3/PS). *Journal of Physics and Chemistry of Solids* **117**, 49–59. https://doi.org/10.1016/j.jpcs.2018.02.009.

Kim, C., Ahn, J. Y., Kim, T. Y., Shin, W. S. & Hwang, I. 2018 Activation of persulfate by nanosized zero-valent iron (NZVI): mechanisms and transformation products of NZVI. *Environmental Science & Technology* **52** (6), 3625–3633. https://doi.org/10.1021/acs.est.7b05847.

Klamerth, N., Malato, S., Agüera, A. & Fernández-Alba, A. 2013 Photo-Fenton and modified photo-Fenton at neutral pH for the treatment of emerging contaminants in wastewater treatment plant effluents: a comparison. *Water Research* **47** (2), 833–840. https://doi.org/10.1016/j.watres.2012.11.008.

Kusic, H., Peternel, I., Ukic, S., Koprivanac, N., Bolanca, T., Papic, S. & Bozic, A. L. 2011 Modeling of iron activated persulfate oxidation treating reactive azo dye in water matrix. *Chemical Engineering Journal* **172** (1), 109–121. https://doi.org/10.1016/j.cej.2011.05.076.

Leng, Y., Guo, W., Shi, X., Li, Y. & Xing, L. 2013 Polyhydroquinone-coated Fe_3O_4 nanocatalyst for degradation of rhodamine B based on sulfate radicals. *Industrial & Engineering Chemistry Research* **52** (38), 13607–13612. https://doi.org/10.1021/ie4015777.

Leng, Y., Guo, W., Shi, X., Li, Y., Wang, A., Hao, F. & Xing, L. 2014 Degradation of Rhodamine B by persulfate activated with Fe_3O_4: effect of polyhydroquinone serving as an electron shuttle. *Chemical Engineering Journal* **240**, 338–343. https://doi.org/10.1016/j.cej.2013.11.090.

Li, H., Wan, J., Ma, Y., Huang, M., Wang, Y. & Chen, Y. 2014 New insights into the role of zero-valent iron surface oxidation layers in persulfate oxidation of dibutyl phthalate solutions. *Chemical Engineering Journal* **250**, 137–147. https://doi.org/10.1016/j.cej.2014.03.092.

Li, H., Wan, J., Ma, Y., Wang, Y. & Guan, Z. 2015 Role of inorganic ions and dissolved natural organic matters on persulfate oxidation of acid orange 7 with zero-valent iron. *RSC Advances* **5** (121), 99935–99943. https://doi.org/10.1039/C5RA16094D.

Li, J., Ji, Q., Lai, B. & Yuan, D. 2017a Degradation of p-nitrophenol by Fe^0/H_2O_2/persulfate system: optimization, performance and mechanisms. *Journal of the Taiwan Institute of Chemical Engineers* **80**, 686–694. https://doi.org/10.1016/j.jtice.2017.09.002.

Li, M., Yang, X., Wang, D. & Yuan, J. 2017b Enhanced oxidation of erythromycin by persulfate activated iron powder–H_2O_2 system: role of the surface Fe species and synergistic effect of hydroxyl and sulfate radicals. *Chemical Engineering Journal* **317**, 103–111. https://doi.org/10.1016/j.cej.2016.12.126.

Li, X., Zhou, M., Pan, Y. & Xu, L. 2017c Pre-magnetized Fe^0/persulfate for notably enhanced degradation and dechlorination of 2, 4-dichlorophenol. *Chemical Engineering Journal* **307**, 1092–1104. https://doi.org/10.1016/j.cej.2016.08.140.

Liang, C. & Guo, Y. Y. 2010 Mass transfer and chemical oxidation of naphthalene particles with zerovalent iron activated persulfate. *Environmental Science & Technology* **44** (21), 8203–8208. https://doi.org/10.1021/es903411a.

Lin, C. C. & Chen, Y. H. 2018 Feasibility of using nanoscale zero-valent iron and persulfate to degrade sulfamethazine in aqueous solutions. *Separation and Purification Technology* **194**, 388–395. https://doi.org/10.1016/j.seppur.2017.10.073.

Liu, C. & Wu, B. 2018 Sulfate radical-based oxidation for sludge treatment: a review. *Chemical Engineering Journal* **335**, 865–875. https://doi.org/10.1016/j.cej.2017.10.162.

Liu, C. S., Shih, K., Sun, C. X. & Wang, F. 2012 Oxidative degradation of propachlor by ferrous and copper ion activated persulfate. *Science of the Total Environment* **416**, 507–512. https://doi.org/10.1016/j.scitotenv.2011.12.004.

Liu, H., Bruton, T. A., Doyle, F. M. & Sedlak, D. L. 2014 In situ chemical oxidation of contaminated groundwater by persulfate: decomposition by Fe (III)-and Mn (IV)-containing oxides and aquifer materials. *Environmental Science & Technology* **48** (17), 10330–10336. https://doi.org/10.1021/es502056d.

Liu, C. M., Diao, Z. H., Huo, W. Y., Kong, L. J. & Du, J. J. 2018 Simultaneous removal of Cu^{2+} and bisphenol A by a novel biochar-supported zero valent iron from aqueous solution: synthesis, reactivity and mechanism. *Environmental Pollution* **239**, 698–705. https://doi.org/10.1016/j.envpol.2018.04.084.

Long, A., Lei, Y. & Zhang, H. 2014 Degradation of toluene by a selective ferrous ion activated persulfate oxidation process. *Industrial & Engineering Chemistry Research* **53** (3), 1033–1039. https://doi.org/10.1021/ie402633n.

Luo, H., Lin, Q., Zhang, X., Huang, Z., Liu, S., Jiang, J., Xiao, R. & Liao, X. 2019 New insights into the formation and transformation of active species in nZVI/BC activated persulfate in alkaline solutions. *Chemical Engineering Journal* **359**, 1215–1223. https://doi.org/10.1016/j.cej.2018.11.056.

Matzek, L. W. & Carter, K. E. 2016 Activated persulfate for organic chemical degradation: a review. *Chemosphere* **151**, 178–188. https://doi.org/10.1016/j.chemosphere.2016.02.055.

Mueller, N. C., Braun, J., Bruns, J., Černík, M., Rissing, P., Rickerby, D. & Nowack, B. 2012 Application of nanoscale zero valent iron (NZVI) for groundwater remediation in Europe. *Environmental Science and Pollution Research* **19** (2), 550–558. https://doi.org/10.1007/s11356-011-0576-3.

Naim, S. & Ghauch, A. 2016 Ranitidine abatement in chemically activated persulfate systems: assessment of industrial iron

waste for sustainable applications. *Chemical Engineering Journal* **288**, 276–288. https://doi.org/10.1016/j.cej.2015.11.101.

Neyens, E. & Baeyens, J. 2003 A review of classic Fenton's peroxidation as an advanced oxidation technique. *Journal of Hazardous Materials* **98** (1–3), 33–50. https://doi.org/10.1016/S0304-3894(02)00282-0.

Nidheesh, P. V. & Gandhimathi, R. 2012 Trends in electro-Fenton process for water and wastewater treatment: an overview. *Desalination* **299**, 1–15. https://doi.org/10.1016/j.desal.2012.05.011.

Nie, M., Yan, C., Li, M., Wang, X., Bi, W. & Dong, W. 2015 Degradation of chloramphenicol by persulfate activated by Fe^{2+} and zerovalent iron. *Chemical Engineering Journal* **279**, 507–515. https://doi.org/10.1016/j.cej.2015.05.055.

Nie, M., Yan, C., Xiong, X., Wen, X., Yang, X. & Dong, W. 2018 Degradation of chloramphenicol using a combination system of simulated solar light, Fe^{2+} and persulfate. *Chemical Engineering Journal* **348**, 455–463. https://doi.org/10.1016/j.cej.2018.04.124.

Niu, C. G., Wang, Y., Zhang, X. G., Zeng, G. M., Huang, D. W., Ruan, M. & Li, X. W. 2012 Decolorization of an azo dye Orange G in microbial fuel cells using Fe (II)-EDTA catalyzed persulfate. *Bioresource Technology* **126**, 101–106. https://doi.org/10.1016/j.biortech.2012.09.001.

Nowack, B. 2002 Environmental chemistry of aminopolycarboxylate chelating agents. *Environmental Science & Technology* **36** (19), 4009–4016. https://doi.org/10.1021/es025683s.

Oh, W. D. & Lim, T. T. 2019 Design and application of heterogeneous catalysts as peroxydisulfate activator for organics removal: an overview. *Chemical Engineering Journal* **358**, 110–133. https://doi.org/10.1016/j.cej.2018.09.203.

Oh, S. Y., Kim, H. W., Park, J. M., Park, H. S. & Yoon, C. 2009 Oxidation of polyvinyl alcohol by persulfate activated with heat, Fe^{2+}, and zero-valent iron. *Journal of Hazardous Materials* **168** (1), 346–351. https://doi.org/10.1016/j.jhazmat.2009.02.065.

Oh, S. Y., Kang, S. G. & Chiu, P. C. 2010 Degradation of 2, 4-dinitrotoluene by persulfate activated with zero-valent iron. *Science of the Total Environment* **408** (16), 3464–3468. https://doi.org/10.1016/j.scitotenv.2010.04.032.

Oh, W. D., Dong, Z. & Lim, T. T. 2016 Generation of sulfate radical through heterogeneous catalysis for organic contaminants removal: current development, challenges and prospects. *Applied Catalysis B: Environmental* **194**, 169–201. https://doi.org/10.1016/j.apcatb.2016.04.003.

Olmez-Hanci, T. & Arslan-Alaton, I. 2013 Comparison of sulfate and hydroxyl radical based advanced oxidation of phenol. *Chemical Engineering Journal* **224**, 10–16. https://doi.org/10.1016/j.cej.2012.11.007.

Olmez-Hanci, T., Arslan-Alaton, I. & Genc, B. 2013 Bisphenol A treatment by the hot persulfate process: oxidation products and acute toxicity. *Journal of Hazardous Materials* **263**, 283–290. https://doi.org/10.1016/j.jhazmat.2013.01.032.

Pan, Y., Zhou, M., Li, X., Xu, L., Tang, Z., Sheng, X. & Li, B. 2017 Highly efficient persulfate oxidation process activated with pre-magnetization Fe^0. *Chemical Engineering Journal* **318**, 50–56. https://doi.org/10.1016/j.cej.2016.05.001.

Park, J. H., Wang, J. J., Tafti, N. & Delaune, R. D. 2019 Removal of Eriochrome Black T by sulfate radical generated from Fe-impregnated biochar/persulfate in Fenton-like reaction. *Journal of Industrial and Engineering Chemistry* **71**, 201–209. https://doi.org/10.1016/j.jiec.2018.11.026.

Pouran, S. R., Aziz, A. A. & Daud, W. M. A. W. 2015 Review on the main advances in photo-Fenton oxidation system for recalcitrant wastewaters. *Journal of Industrial and Engineering Chemistry* **21**, 53–69. https://doi.org/10.1016/j.jiec.2014.05.005.

Pu, M., Ma, Y., Wan, J., Wang, Y., Huang, M. & Chen, Y. 2014 Fe/S doped granular activated carbon as a highly active heterogeneous persulfate catalyst toward the degradation of Orange G and diethyl phthalate. *Journal of Colloid and Interface Science* **418**, 330–337. https://doi.org/10.1016/j.jcis.2013.12.034.

Pulicharla, R., Drouinaud, R., Brar, S. K., Drogui, P., Proulx, F., Verma, M. & Surampalli, R. Y. 2018 Activation of persulfate by homogeneous and heterogeneous iron catalyst to degrade chlortetracycline in aqueous solution. *Chemosphere* **207**, 543–551. https://doi.org/10.1016/j.chemosphere.2018.05.134.

Rao, Y. F., Qu, L., Yang, H. & Chu, W. 2014 Degradation of carbamazepine by Fe (II)-activated persulfate process. *Journal of Hazardous Materials* **268**, 23–32. https://doi.org/10.1016/j.jhazmat.2014.01.010.

Ravikumar, K. V. G., Santhosh, S., Sudakaran, S. V., Nancharaiah, Y. V., Mrudula, P., Chandrasekaran, N. & Mukherjee, A. 2018 Biogenic nano zero valent iron (Bio-nZVI) anaerobic granules for textile dye removal. *Journal of Environmental Chemical Engineering* **6** (2), 1683–1689. https://doi.org/10.1016/j.jece.2018.02.023.

Rodriguez, S., Vasquez, L., Costa, D., Romero, A. & Santos, A. 2014 Oxidation of Orange G by persulfate activated by Fe (II), Fe (III) and zero valent iron (ZVI). *Chemosphere* **101**, 86–92. https://doi.org/10.1016/j.chemosphere.2013.12.037.

Satapanajaru, T., Yoo-iam, M., Bongprom, P. & Pengthamkeerati, P. 2015 Decolorization of Reactive Black 5 by persulfate oxidation activated by ferrous ion and its optimization. *Desalination and Water Treatment* **56** (1), 121–135. https://doi.org/10.1080/19443994.2014.932710.

Shang, W., Dong, Z., Li, M., Song, X., Zhang, M., Jiang, C. & Feiyun, S. 2019 Degradation of diatrizoate in water by Fe (II)-activated persulfate oxidation. *Chemical Engineering Journal* **361**, 1333–1344. https://doi.org/10.1016/j.cej.2018.12.139.

Song, Q., Feng, Y., Liu, G. & Lv, W. 2019 Degradation of the flame retardant triphenyl phosphate by ferrous ion-activated hydrogen peroxide and persulfate: kinetics, pathways, and mechanisms. *Chemical Engineering Journal* **361**, 929–936. https://doi.org/10.1016/j.cej.2018.12.140.

Soubh, A. M., Baghdadi, M., Abdoli, M. A. & Aminzadeh, B. 2018 Zero-valent iron nanofibers (ZVINFs) immobilized on the surface of reduced ultra-large graphene oxide (rULGO) as a persulfate activator for treatment of landfill leachate. *Journal of Environmental Chemical Engineering* **6** (5), 6568–6579. https://doi.org/10.1016/j.jece.2018.10.011.

Stefaniuk, M., Oleszczuk, P. & Ok, Y. S. 2016 Review on nano zerovalent iron (nZVI): from synthesis to environmental applications. *Chemical Engineering Journal* **287**, 618–632. https://doi.org/10.1016/j.cej.2015.11.046.

Sun, C., Zhou, R., Jianan, E., Sun, J., Su, Y. & Ren, H. 2016 Ascorbic acid-coated Fe_3O_4 nanoparticles as a novel heterogeneous catalyst of persulfate for improving the degradation of 2,4-dichlorophenol. *RSC Advances* **6** (13), 10633–10640. https://doi.org/10.1039/C5RA22491H.

Tan, X. F., Liu, Y. G., Gu, Y. L., Xu, Y., Zeng, G. M., Hu, X. J., Liu, S. B., Wang, X., Liu, X. M. & Li, J. 2016 Biochar-based nanocomposites for the decontamination of wastewater: a review. *Bioresource Technology* **212**, 318–333. https://doi.org/10.1016/j.biortech.2016.04.093.

Teel, A. L., Ahmad, M. & Watts, R. J. 2011 Persulfate activation by naturally occurring trace minerals. *Journal of Hazardous Materials* **196**, 153–159. https://doi.org/10.1016/j.jhazmat.2011.09.011.

Temiz, K., Olmez-Hanci, T. & Arslan-Alaton, I. 2016 Zero-valent iron-activated persulfate oxidation of a commercial alkyl phenol polyethoxylate. *Environmental Technology* **37** (14), 1757–1767. https://doi.org/10.1080/09593330.2015.1131751.

Tsitonaki, A., Petri, B., Crimi, M., Mosbæk, H., Siegrist, R. L. & Bjerg, P. L. 2010 In situ chemical oxidation of contaminated soil and groundwater using persulfate: a review. *Critical Reviews in Environmental Science and Technology* **40** (1), 55–91. https://doi.org/10.1080/10643380802039303.

Wacławek, S., Lutze, H. V., Grübel, K., Padil, V. V., Černík, M. & Dionysiou, D. D. 2017 Chemistry of persulfates in water and wastewater treatment: a review. *Chemical Engineering Journal* **330**, 44–62. https://doi.org/10.1016/j.cej.2017.07.132.

Wang, S. & Wang, J. 2017 Comparative study on sulfamethoxazole degradation by Fenton and Fe (II)-activated persulfate process. *RSC Advances* **7** (77), 48670–48677. https://doi.org/10.1039/C7RA09325 J.

Wang, S. & Wang, J. 2018 Trimethoprim degradation by Fenton and Fe (II)-activated persulfate processes. *Chemosphere* **191**, 97–105. https://doi.org/10.1016/j.chemosphere.2017.10.040.

Wang, X., Wang, L., Li, J., Qiu, J., Cai, C. & Zhang, H. 2014 Degradation of Acid Orange 7 by persulfate activated with zero valent iron in the presence of ultrasonic irradiation. *Separation and Purification Technology* **122**, 41–46. https://doi.org/10.1016/j.seppur.2013.10.037.

Wang, C., Wan, J., Ma, Y. & Wang, Y. 2016a Insights into the synergy of zero-valent iron and copper oxide in persulfate oxidation of Orange G solutions. *Research on Chemical Intermediates* **42** (2), 481–497. https://doi.org/10.1007/s11164-015-2035-0.

Wang, Q., Shao, Y., Gao, N., Chu, W., Deng, J., Shen, X., Lu, X., Zhu, Y. & Wei, X. 2016b Degradation of alachlor with zero-valent iron activating persulfate oxidation. *Journal of the Taiwan Institute of Chemical Engineers* **63**, 379–385. https://doi.org/10.1016/j.jtice.2016.03.038.

Wang, Y., Chen, S. Y., Yang, X., Huang, X. F., Yang, Y. H., He, E. K., Wang, X. Q. & Qiu, R. L. 2017 Degradation of 2, 2′, 4, 4′-tetrabromodiphenyl ether (BDE-47) by a nano zerovalent iron-activated persulfate process: the effect of metal ions. *Chemical Engineering Journal* **317**, 613–622. https://doi.org/10.1016/j.cej.2017.02.070.

Wang, X., Du, Y., Liu, H. & Ma, J. 2018 Ascorbic acid/Fe^0 composites as an effective persulfate activator for improving the degradation of rhodamine B. *RSC Advances* **8** (23), 12791–12798. https://doi.org/10.1039/C8RA01506F.

Wang, H., Guo, W., Yin, R., Du, J., Wu, Q., Luo, H., Liu, B., Sseguya, F. & Ren, N. 2019a Biochar-induced Fe (III) reduction for persulfate activation in sulfamethoxazole degradation: insight into the electron transfer, radical oxidation and degradation pathways. *Chemical Engineering Journal* **362**, 561–569. https://doi.org/10.1016/j.cej.2019.01.053.

Wang, L., Wang, Y., Ma, F., Tankpa, V., Bai, S., Guo, X. & Wang, X. 2019b Mechanisms and reutilization of modified biochar used for removal of heavy metals from wastewater: a review. *Science of the Total Environment*. https://doi.org/10.1016/j.scitotenv.2019.03.011.

Wang, S., Wu, J., Lu, X., Xu, W., Gong, Q., Ding, J., Dan, B. & Xie, P. 2019c Removal of acetaminophen in the Fe^{2+}/persulfate system: kinetic model and degradation pathways. *Chemical Engineering Journal* **358**, 1091–1100. https://doi.org/10.1016/j.cej.2018.09.145.

Wang, S., Zhao, M., Zhou, M., Li, Y. C., Wang, J., Gao, B., Sato, S., Feng, K., Yin, W., Igalavithana, A. D., Oleszczuk, P., Wang, X. & Ok, X. 2019d Biochar-supported nZVI (nZVI/BC) for contaminant removal from soil and water: a critical review. *Journal of Hazardous Materials* **373**, 820–834. https://doi.org/10.1016/j.jhazmat.2019.03.080.

Wei, X., Gao, N., Li, C., Deng, Y., Zhou, S. & Li, L. 2016 Zero-valent iron (ZVI) activation of persulfate (PS) for oxidation of bentazon in water. *Chemical Engineering Journal* **285**, 660–670. https://doi.org/10.1016/j.cej.2015.08.120.

Wei, D., Li, B., Huang, H., Luo, L., Zhang, J., Yang, Y., Guo, J., Tang, L., Zeng, G. & Zhou, Y. 2018 Biochar-based functional materials in the purification of agricultural wastewater: fabrication, application and future research needs. *Chemosphere* **197**, 165–180. https://doi.org/10.1016/j.chemosphere.2017.12.193.

Weng, C. H. & Tsai, K. L. 2016 Ultrasound and heat enhanced persulfate oxidation activated with Fe0 aggregate for the decolorization of CI Direct Red 23. *Ultrasonics Sonochemistry* **29**, 11–18. https://doi.org/10.1016/j.ultsonch.2015.08.012.

Weng, C. H. & Tao, H. 2018 Highly efficient persulfate oxidation process activated with Fe0 aggregate for decolorization of reactive azo dye Remazol Golden Yellow. *Arabian Journal of Chemistry* **11** (8), 1292–1300. https://doi.org/10.1016/j.arabjc.2015.05.012.

Weng, C. H., Ding, F., Lin, Y. T. & Liu, N. 2015 Effective decolorization of polyazo direct dye Sirius Red F3B using persulfate activated with Fe^0 aggregate. *Separation and Purification Technology* **147**, 147–155. https://doi.org/10.1016/j.seppur.2015.03.062.

Wu, X., Gu, X., Lu, S., Qiu, Z., Sui, Q., Zang, X., Miao, Z. & Xu, M. 2015 Strong enhancement of trichloroethylene

degradation in ferrous ion activated persulfate system by promoting ferric and ferrous ion cycles with hydroxylamine. *Separation and Purification Technology* **147**, 186–193. https://doi.org/10.1016/j.seppur.2015.04.031.

Wu, X., Gu, X., Lu, S., Qiu, Z., Sui, Q., Zang, X., Miao, Z., Xu, M. & Danish, M. 2016 Accelerated degradation of tetrachloroethylene by Fe (II) activated persulfate process with hydroxylamine for enhancing Fe (II) regeneration. *Journal of Chemical Technology & Biotechnology* **91** (5), 1280–1289. https://doi.org/10.1002/jctb.4718.

Wu, S., He, H., Li, X., Yang, C., Zeng, G., Wu, B., He, S. & Lu, L. 2018 Insights into atrazine degradation by persulfate activation using composite of nanoscale zero-valent iron and graphene: performances and mechanisms. *Chemical Engineering Journal* **341**, 126–136. https://doi.org/10.1016/j.cej.2018.01.136.

Wu, J., Wang, B., Blaney, L., Peng, G., Chen, P., Cui, Y., Deng, S., Wang, Y., Huang, J. & Yu, G. 2019 Degradation of sulfamethazine by persulfate activated with organo-montmorillonite supported nano-zero valent iron. *Chemical Engineering Journal* **361**, 99–108. https://doi.org/10.1016/j.cej.2018.12.024.

Xiao, R., Luo, Z., Wei, Z., Luo, S., Spinney, R., Yang, W. & Dionysiou, D. D. 2018 Activation of peroxymonosulfate/persulfate by nanomaterials for sulfate radical-based advanced oxidation technologies. *Current Opinion in Chemical Engineering* **19**, 51–58. https://doi.org/10.1016/j.coche.2017.12.005.

Xiao, S., Cheng, M., Zhong, H., Liu, Z., Liu, Y., Yang, X. & Liang, Q. 2019 Iron-mediated activation of persulfate and peroxymonosulfate in both homogeneous and heterogeneous ways: a review. *Chemical Engineering Journal*. https://doi.org/10.1016/j.cej.2019.123265

Xu, X. R. & Li, X. Z. 2010 Degradation of azo dye Orange G in aqueous solutions by persulfate with ferrous ion. *Separation and Purification Technology* **72** (1), 105–111. https://doi.org/10.1016/j.seppur.2010.01.012.

Xu, H., Tian, W., Zhang, Y., Tang, J., Zhao, Z. & Chen, Y. 2018a Reduced graphene oxide/attapulgite-supported nanoscale zero-valent iron removal of acid red 18 from aqueous solution. *Water, Air, & Soil Pollution* **229** (12), 388. https://doi.org/10.1007/s11270-018-4033-5.

Xu, J., Zhang, X., Sun, C., He, H., Dai, Y., Yang, S., Lin, Y., Zhan, X., Li, Q. & Zhou, Y. 2018b Catalytic degradation of diatrizoate by persulfate activation with peanut shell biochar-supported nano zero-valent iron in aqueous solution. *International Journal of Environmental Research and Public Health* **15** (9), 1937. https://doi.org/10.3390/technologies8010012.

Yahya, M. S., Oturan, N., El Kacemi, K., El Karbane, M., Aravindakumar, C. T. & Oturan, M. A. 2014 Oxidative degradation study on antimicrobial agent ciprofloxacin by electro-Fenton process: kinetics and oxidation products. *Chemosphere* **117**, 447–454. https://doi.org/10.1016/j.chemosphere.2014.08.016.

Yan, J., Lei, M., Zhu, L., Anjum, M. N., Zou, J. & Tang, H. 2011 Degradation of sulfamonomethoxine with Fe_3O_4 magnetic nanoparticles as heterogeneous activator of persulfate. *Journal of Hazardous Materials* **186** (2–3), 1398–1404. https://doi:10.1016/j.jhazmat.2010.12.017.

Yan, J., Han, L., Gao, W., Xue, S. & Chen, M. 2015 Bidochar supported nanoscale zerovalent iron composite used as persulfate activator for removing trichloroethylene. *Bioresource Technology* **175**, 269–274. https://doi.org/10.1016/j.biortech.2014.10.103.

Yang, S. & Che, D. 2017 Degradation of aquatic sulfadiazine by Fe^0/persulfate: kinetics, mechanisms, and degradation pathway. *RSC Advances* **7** (67), 42233–42241. https://doi.org/10.1039/C7RA07920F.

Yang, B., Tian, Z., Zhang, L., Guo, Y. & Yan, S. 2015 Enhanced heterogeneous Fenton degradation of Methylene Blue by nanoscale zero valent iron (nZVI) assembled on magnetic Fe_3O_4/reduced graphene oxide. *Journal of Water Process Engineering* **5**, 101–111. https://doi.org/10.1016/j.jwpe.2015.01.006.

Yu, S., Gu, X., Lu, S., Xue, Y., Zhang, X., Xu, M., Qiu, Z. & Sui, Q. 2018 Degradation of phenanthrene in aqueous solution by a persulfate/percarbonate system activated with CA chelated-Fe (II). *Chemical Engineering Journal* **333**, 122–131. https://doi.org/10.1016/j.cej.2017.09.158.

Yuan, Y., Tao, H., Fan, J. & Ma, L. 2015 Degradation of p-chloroaniline by persulfate activated with ferrous sulfide ore particles. *Chemical Engineering Journal* **268**, 38–46. https://doi.org/10.1016/j.cej.2014.12.092.

Zhang, H., Wang, Z., Liu, C., Guo, Y., Shan, N., Meng, C. & Sun, L. 2014 Removal of COD from landfill leachate by an electro/Fe^{2+}/peroxydisulfate process. *Chemical Engineering Journal* **250**, 76–82. https://doi.org/10.1016/j.cej.2014.03.114.

Zhang, B. T., Zhang, Y., Teng, Y. & Fan, M. 2015a Sulfate radical and its application in decontamination technologies. *Critical Reviews in Environmental Science and Technology* **45** (16), 1756–1800. https://doi.org/10.1080/10643389.2014.970681.

Zhang, M., Chen, X., Zhou, H., Murugananthan, M. & Zhang, Y. 2015b Degradation of p-nitrophenol by heat and metal ions co-activated persulfate. *Chemical Engineering Journal* **264**, 39–47. https://doi.org/10.1016/j.cej.2014.11.060.

Zhang, Y., Tran, H. P., Du, X., Hussain, I., Huang, S., Zhou, S. & Wen, W. 2017 Efficient pyrite activating persulfate process for degradation of p-chloroaniline in aqueous systems: a mechanistic study. *Chemical Engineering Journal* **308**, 1112–1119. https://doi.org/10.1016/j.cej.2016.09.104.

Zhang, D., Li, Y., Tong, S., Jiang, X., Wang, L., Sun, X., Li, J., Liu, X. & Shen, J. 2018a Biochar supported sulfide-modified nanoscale zero-valent iron for the reduction of nitrobenzene. *RSC Advances* **8** (39), 22161–22168. https://doi.org/10.1039/C8RA04314 K.

Zhang, K., Zhou, X., Zhang, T., Yu, L., Qian, Z., Liao, W. & Li, C. 2018b Degradation of the earthy and musty odorant 2, 4, 6-tricholoroanisole by persulfate activated with iron of different valences. *Environmental Science and Pollution Research* **25** (4), 3435–3445. https://doi.org/10.1007/s11356-017-0452-x.

Zhang, Y., Zhang, Q., Dong, Z. & Hong, J. 2018c Degradation of acetaminophen with ferrous/copperoxide activate persulfate: synergism of iron and copper. *Water Research* **146**, 232–243. https://doi.org/10.1016/j.watres.2018.09.028.

Zhao, J., Zhang, Y., Quan, X. & Chen, S. 2010 Enhanced oxidation of 4-chlorophenol using sulfate radicals generated from zero-valent iron and peroxydisulfate at ambient temperature. *Separation and Purification Technology* **71** (3), 302–307. https://doi.org/10.1016/j.seppur.2009.12.010.

Zhao, L., Hou, H., Fujii, A., Hosomi, M. & Li, F. 2014 Degradation of 1, 4-dioxane in water with heat-and Fe^{2+}-activated persulfate oxidation. *Environmental Science and Pollution Research* **21** (12), 7457–7465. https://doi.org/10.1007/s11356-014-2668-3.

Zhou, L., Ma, J., Zhang, H., Shao, Y. & Li, Y. 2015 Fabrication of magnetic carbon composites from peanut shells and its application as a heterogeneous Fenton catalyst in removal of methylene blue. *Applied Surface Science* **324**, 490–498. https://doi.org/10.1016/j.apsusc.2014.10.152.

Zhou, L., Zheng, W., Ji, Y., Zhang, J., Zeng, C., Zheng, Y., Wang, Q. & Yang, X. 2013 Ferrous-activated persulfate oxidation of arsenic (III) and diuron in aquatic system. *Journal of Hazardous Materials* **263**, 422–430. https://doi.org/10.1016/j.jhazmat.2013.09.056.

Zhu, C., Fang, G., Dionysiou, D. D., Liu, C., Gao, J., Qin, W. & Zhou, D. 2016 Efficient transformation of DDTs with persulfate activation by zero-valent iron nanoparticles: a mechanistic study. *Journal of Hazardous Materials* **316**, 232–241. https://doi.org/10.1016/j.jhazmat.2016.05.040.

Zhu, Y., Yue, M., Natarajan, V., Kong, L., Ma, L., Zhang, Y., Zhao, Q. & Zhan, J. 2018 Efficient activation of persulfate by Fe_3O_4 @ β-cyclodextrin nanocomposite for removal of bisphenol A. *RSC Advances* **8** (27), 14879–14887. https://doi.org/10.1039/C8RA01696H.

Zou, X., Zhou, T., Mao, J. & Wu, X. 2014 Synergistic degradation of antibiotic sulfadiazine in a heterogeneous ultrasound-enhanced Fe^0/persulfate Fenton-like system. *Chemical Engineering Journal* **257**, 36–44. https://doi.org/10.1016/j.cej.2014.07.048.

First received 29 January 2020; accepted in revised form 7 April 2020. Available online 20 April 2020